IPP-Report

Max-Planck-Institut
für Plasmaphysik

Ya.I. Kolesnichenko, V.V. Lutsenko, A. Weller,
H. Wobig, Yu.V. Yakovenko

Alfvén eigenmodes in Helias configurations (part II)

IPP III/271

July 2002

Ya.I. Kolesnichenko, V.V. Lutsenko, A. Weller,
H. Wobig, Yu.V. Yakovenko

Alfvén eigenmodes in Helias configurations (part II)

IPP III/271
July 2002

Alfvén eigenmodes in Helias configurations (part II)

Ya. I. Kolesnichenko*, V. V. Lutsenko*, A. Weller**,

H. Wobig**, Yu. V. Yakovenko*

*Institute for Nuclear Research, Prospekt Nauky 47, 03680 Kyiv, Ukraine

**Max-Planck Institut für Plasmaphysik, IPP-EURATOM Association,

D-85748 Garching bei München, Germany

(June 7, 2002)

Abstract

An equation for the Alfvén eigenmodes (AE) derived in the work *Ya. I. Kolesnichenko, V. V. Lutsenko, H. Wobig, Yu. V. Yakovenko, and O. P. Fesenyuk, Alfvén eigenmodes in Helias configurations (part I), Report IPP III/261 (2000)* is generalized to include effects of plasma rotation and relatively large magnitude of coupling parameters associated with strong plasma shaping. It is shown that the Doppler frequency shift is "shared" by Fourier harmonics that compose the gap modes. A new gap in the Alfvén continuum (AC) associated with the shear of the rotation is predicted. It is demonstrated that keeping all terms with large coupling parameters considerably changes the spectrum of the AEs residing in the corresponding gap of AC. Resonances between energetic ions and AEs are analyzed. The existence of "compound resonances" associated with the compound structure of gap modes is predicted. An expression for the instability growth rate taking into account such a resonance is derived. Peculiarities of the gap modes and the Global Alfvén Eigenmodes (GAE) are discussed. It is concluded that the GAEs can exist only in the low-frequency part of the Alfvén spectrum in Wendelstein 7-AS. An explanation of the experimentally observed temporal evolution of Alfvénic activity in experiments on W7-AS is suggested.

I. INTRODUCTION

In a previous work of the authors[1] (see also Ref.[2]) an equation for Alfvén Eigenmodes (AE) in the optimized stellarators of the Wendelstein line (Helias configurations) was derived and analyzed. Two codes were developed: first, the code COBRA (COntinuum BRanches of Alfvén waves) intended for investigating the Alfvén continuum; second, the code BOA (Branches Of Alfvén modes) for the calculation of discrete eigenmodes. It was shown that there exist absolute gaps in the Alfvén continuum, where there are no continuum branches. The existence of specific gaps in the continuum of Helias configurations, where discrete modes may reside, was predicted. In particular, it was shown that the rotation of the strongly elongated plasma cross section along the large azimuth of the torus produces the widest gap in the continuum, so-called HAE_{21} gap (HAE means "Helicity-induced Alfvén Eigenmodes"; the subscripts 2 and 1 denote the poloidal and toroidal coupling numbers, respectively); the modulation of the elongation and the mirror Fourier harmonic of the magnetic field strength result in the MAE gap containing the MAE modes (Mirror-induced Alfvén Eigenmodes). Later a theory of the resonance destabilization of Alfvén eigenmodes by energetic circulating ions was developed.[3] It was found that specific wave-particle resonances do exist in stellarators, which may strongly enhance the instabilities and change the conditions of the wave destabilization. The predicted resonances may play an important role when nonaxisymmetric harmonics (e.g., a helical one) in the Fourier spectrum of the magnetic field strength rather than toroidicity have a dominant influence on the particle drift motion. In addition to these results based on the description of the bulk plasma in the framework of the ideal MHD, a study of non-ideal effects on Alfvén instabilities in the Wendelstein-line stellarators was started in Ref.[4].

Note that the existence of MAE modes and HAE modes in the Wendelstein-line stellarators was shown also by using the CAS3D stability code based on the full set of the ideal MHD equations.[5,6] For other types of helical devices the HAE modes were considered in Ref.[7]. On the basis of CAS3D calculations, an Alfvénic activity at the frequency about 50 kHz observed in experiments with Neutral Beam Injection (NBI) on W7-AS (Wendel-

stein 7-AS[8]) was identified as the instability of TAE modes (Toroidicity-induced Alfvén Eigenmodes). The presence of energetic ions was not taken into account by the CAS3D code. Therefore, a new code, CAS3D-K, is now developed to include the response of the energetic ions.[9] On the other hand, there was an attempt to interpret experimental results from W7-AS using the gyrofluid code FAR, which, however, assumed that the energetic ions have the Maxwellian velocity distribution.[10] Although the mentioned works explain some experimental data, no attempts have been done yet to understand why sometimes the frequencies of the destabilized Alfvén waves lie in the wide range from 50 kHz to 500 kHz, but in other cases the frequency range is very narrow.[11] Moreover, it is not clear why sometimes even a small change of the Alfvén velocity strongly affects the character of the Alfvénic activity in W7-AS.[11]

The purposes of this work are to develop further the theory of Refs.[1–3] and to interpret the mentioned experimental observations on W7-AS. In particular, the work includes studies of features of the gap modes and the Global Alfvén Eigenmodes GAE), the effect of the complexity of gap modes on the resonances of the gap modes and energetic ions, the influence of the plasma rotation and the large magnitude of some coupling parameters on the gap modes etc. An attempt is made to explain the temporal evolution of the Alfvén activity in the shot #43368 of W7-AS. The analysis in the work is carried out in the assumption that the plasma is incompressible. This assumption is justified due to the fact that finite compressibility influences mainly the low-frequency part of the Alfvén continuum, and even that part is relatively weakly changed (e.g., the TAE gap is shifted up by about 12%).[12]

The structure of the work is as follows. In Sec. II distinctive features of the gap modes and the GAE modes are discussed; the Alfvén continuum in W7-AS is calculated and analyzed. In Sec. III the resonances between the gap modes and the energetic ions are studied. In Sec. IV experimental data on Alfvénic activity obtained on W7-AS are described, and the developed theory is applied to explain them. Section V deals with effects of plasma rotation. Here, an equation for AEs in a rotating plasma is derived and analyzed. In Sec. VI an equation for the gap modes associated with strong plasma

shaping is derived, where all terms with the coupling parameters are kept (in contrast to a corresponding equation in Refs.[1,2], where all such terms were neglected except for the term with the second radial derivative of the wave function). It is solved numerically for the HAE_{21} modes. Section VII summarizes the obtained results.

II. GAP MODES AND GLOBAL ALFVÉN EIGENMODES. COMPOUND MODES

It is known that the magnetic shear and the plasma inhomogeneity result in the dependence of the Alfvén frequency $\omega_A = |k_\parallel| v_A$ ($k_\parallel$ is the longitudinal wave number, v_A is the Alfvén velocity) on the radial coordinate, r. Therefore, if the plasma were a cylinder, $\omega_A(r)$ would describe an Alfvén continuum (AC). Then the only possible AEs would be the GAE modes. The eigenfrequencies of a GAE lies just below a minimum of $\omega_A(r)$, and its eigenfunction usually has a maximum near the radius where $\omega_A(r)$ has a minimum.[13,14] The situation changes in toroidal systems. First, a monochromatic (i.e., consisting of the only Fourier harmonic) GAE becomes non-monochromatic because of the presence of coupling factors (associated with the break of the poloidal and toroidal symmetries); nevertheless, there is a dominant $k_\parallel$, which is the same as in the cylindrical geometry. Therefore, one can say that GAEs are approximately monochromatic. Second, which is very important, there exist gaps in AC of toroidal systems, where other discrete AEs (TAE, HAE, MAE etc.) can reside.[15,7,1,6] In contrast to GAEs, the gap modes are essentially non-monochromatic: They appear only as a result of superposition of one or more pairs of waves propagating in opposite directions.

Considerable plasma shaping and the absence of the axial symmetry strongly complicate AC in stellarators.[16] Because of this, one often uses a simplified picture of AC in a particular discharge, e.g., calculates families of $\omega_A(r)$ having minima at certain radii, from which it follows that GAEs can exist in the considered discharge. However, below we will show that such an approach may be not justified. We will discuss also general features of AC and AEs in stellarators and consider a specific example relevant to W7-AS.

We proceed from the following equation describing AC:[15,1,2]

$$\hat{L}\left(h_g\hat{L}\Psi\right)+\frac{\omega^2R_0^2}{\bar{v}_A^2}h_c\Psi=0, \tag{1}$$

where ω is the eigenfrequency, Ψ is the scalar potential (the eigenfunction), $h_g=g^{11}/\bar{g}^{11}$, $h_c=h_g/h_B^4$, $h_B=B/\bar{B}$, $g^{11}\equiv|\nabla\psi|^2$ is a component of the contravariant metric tensor, $\bar{g}^{11}=2\bar{\delta}\bar{B}\psi$ is the approximate flux-surface average of g^{11}, $\bar{\delta}$ is the average of $\delta(\varphi)=(\kappa+\kappa^{-1})/2$, κ is the elongation of flux surfaces near the magnetic axis, B is the equilibrium magnetic field, $\bar{B}$ is the average magnetic field at the magnetic axis, $\bar{v}_A=\bar{B}/(4\pi\rho)^{1/2}$, ρ is the mass density of the plasma, $\hat{L}=\iota\partial/\partial\vartheta+\partial/\partial\varphi$ is the operator of differentiation along field lines, ι is the rotational transform, $R_0=L/(2\pi)$ is the major radius of the torus, L is the length of the magnetic axis. When writing the equation, we used the flux coordinate system $(x^1,x^2,x^3)=(\psi,\vartheta,\varphi)$,[17] where ψ is the toroidal magnetic flux; ϑ and φ are the poloidal and toroidal coordinates, respectively. Equation (1) is completed with the natural boundary condition of periodicity. It describes local resonance of Alfvén waves at a "separate" flux surface and includes only differentiation within the flux surface (by angular variables) with ψ considered as a parameter. Therefore, the eigenvalues of the equation are functions of ψ and produce branches of the continuum as ψ is varied.

To analyze Eq. (1), we expand the quantities entering Eq. (1) in Fourier series:

$$\Psi=\sum_{m,n=-\infty}^{\infty}\Psi_{m,n}(r)\exp(im\vartheta-in\varphi-i\omega t), \tag{2}$$

$$h_{g,B,c}=1+\frac{1}{2}\sum_{\mu,\nu=-\infty}^{\infty}\epsilon_{g,B,c}^{(\mu\nu)}(r)\exp(i\mu\vartheta-i\nu N\varphi), \tag{3}$$

where $r=r(\psi)$ is defined by $\psi=\bar{B}r^2/2$, m and n are the poloidal and toroidal mode numbers, N is the number of the field periods along the large azimuth of the torus, $\epsilon_{g,B,c}^{(-\mu,-\nu)}=\epsilon_{g,B,c}^{(\mu\nu)*}$, "$*$" denotes complex conjugate, $\epsilon_c^{(\mu\nu)}\approx\epsilon_g^{(\mu\nu)}-4\epsilon_B^{(\mu\nu)}$ when $\epsilon_{g,B}^{(\mu\nu)}\ll 1$. Then Eq. (1) is reduced to a matrix eigenvalue problem.[2] As one would expect, the non-diagonal elements of these matrices, which allow for the mode coupling, vanish when all Fourier coefficients in Eq. (3) except for $\mu=\nu=0$ are zero. For this reason, we will refer to the parameters $\epsilon_B^{(\mu\nu)}$, $\epsilon_g^{(\mu\nu)}$, and $\epsilon_c^{(\mu\nu)}$ as "coupling parameters corresponding to the coupling numbers μ and ν." The coupling parameters $\epsilon_B^{(\mu\nu)}$ are usually small. In particular, in W7-AS, the dominant harmonics are $\epsilon_t\equiv\epsilon_B^{(10)}$ and $\epsilon_h\equiv\epsilon_B^{(-11)}$, $|\epsilon_t|$

exceeding $|\epsilon_h|$ by a factor of ≈ 1.5, see Fig. 1. In contrast to this, in Wendelstein 7-X[18] and in the reactor projects HSR5/22[19] and HSR4/18[20] (Helias Stellarator Reactors) the mirror harmonic, $\epsilon_B^{(01)}$, dominates, see, e.g., Ref.[3]. The largest of the coupling parameters $\epsilon_g^{(\mu\nu)}$ in all mentioned stellarator configurations is $\epsilon_g^{(21)}$. In many cases it will be convenient to treat $\epsilon_g^{(\mu\nu)}$ as small parameters, too, although some of them, especially, $\epsilon_g^{(21)}$, may be relatively large (for instance, $\epsilon_g^{(21)} = 0.8$ in the 4-period Helias reactor HSR4/18 and 0.5 in W7-AS).

In the simplest case of the cylindrical geometry, when the coefficients of Eq. (1) do not depend on the angular variables, all harmonics $\Psi_{m,n}$ are completely decoupled. Then the continuum consists of the branches $\omega = \pm\omega_{mn}(r) = \pm|k_{mn}|\bar{v}_A$, where $k_{m,n} \equiv k_\parallel(m,n) = (m\iota - n)/R_0$. Hence, the continuum in the cylindrical geometry occupies the whole range of ω (for $m, n = -\infty \ldots \infty$). Thus, the frequency of a GAE arising at a minimum of a continuum branch with certain m and n always lies in the continuum. However, there is no contradiction between this fact and the status of a GAE as a mode of the discrete spectrum because different Fourier harmonics in the cylindrical geometry are completely decoupled, the GAE lying outside the range of the corresponding continuum branch. In a toroidal geometry, the main harmonic of a GAE is coupled to other (satellite) harmonics. Strictly speaking, a GAE in the presence of such coupling does not belong to the discrete spectrum. The coupling results in the energy transfer to local Alfvén resonances [the radii where the GAE frequency crosses satellite continuum branches on the (r, ω) plane].[21] There the energy of the wave is dissipated in some way, which results in damping of the wave (so-called "continuum damping"). Aside from the local Alfvén resonance radii, the amplitudes of the satellite harmonics are relatively small; therefore, a GAE mode has a dominant Fourier harmonic.

This property distinguishes GAEs from the modes residing in the gaps of the continuum. The gaps are produced by various factors that break the cylindrical symmetry and couple Fourier harmonics of the waves with different m and n. The mechanism producing the gaps is the so-called "avoided-crossing phenomenon": As soon as two continuum branches are coupled, the interaction breaks and reconnects them near the points of their

intersection so that the intersection points disappear. Considering only two interacting harmonics of the mode, $(m,n) = (m_1,n_1)$ and $(m,n) = (m_2,n_2) = (m_1+\mu, n_1+\nu N)$, we can reduce Eq. (1) to the following simplified eigenvalue problem:

$$\begin{pmatrix} k_1^2 & \frac{1}{2}\epsilon_g^{(\mu\nu)} k_1 k_2 \\ \frac{1}{2}\epsilon_g^{(\mu\nu)} k_1 k_2 & k_2^2 \end{pmatrix} \begin{pmatrix} \Psi_1 \\ \Psi_2 \end{pmatrix} = \frac{\omega^2}{\bar{v}_A^2} \begin{pmatrix} 1 & \frac{1}{2}\epsilon_c^{(\mu\nu)} \\ \frac{1}{2}\epsilon_c^{(\mu\nu)} & 1 \end{pmatrix} \begin{pmatrix} \Psi_1 \\ \Psi_2 \end{pmatrix}, \tag{4}$$

where $k_j = (m_j\iota - n_j)/R_0$, $j = 1,2$. Having solved this eigenvalue problem, one can see that in the vicinity of the radial points (r_*) where the continua for $\epsilon_g^{(\mu\nu)} = \epsilon_c^{(\mu\nu)} = 0$ would intersect, i.e., $k_1 = \pm k_2$, the solutions for non-zero coupling parameters form gaps. The practically important case is $k_1 = -k_2$. Then the width of the gap is $\Delta\omega \approx |(\epsilon_g^{(\mu\nu)} + \epsilon_c^{(\mu\nu)})k_1|\bar{v}_A/2$. In the new continuum branches formed above and below each gap, the harmonics are strongly mixed, $|\Psi_1| \approx |\Psi_2|$.

The gap modes, which may reside in the gap have a similar harmonic composition: They are dominated (at least, in the vicinity of r_*) by the two harmonics with opposite values of $k_\parallel$.

In spite of the presence of several coupling parameters, the dominant Fourier harmonics of the gap modes are those which are associated with a particular coupling parameter responsible for the gap. To demonstrate it, we consider MAE modes. These modes exist due to the presence of the coupling parameters $\epsilon_{B,g}^{(01)}$, which are considerably less than $\epsilon_g^{(21)}$. This implies that more than two harmonics must be taken into account to calculate the MAE modes.[2] Results of calculations of four dominant MAE harmonics in a homogeneous plasma of the 5-period Helias reactor HSR5/22 with the code BOA are shown in Fig. 2. We observe that the harmonics $E_{m,n}$ and $E_{m,n+5}$ ($E \equiv \Phi/r$, Φ is the scalar potential of the eigenmode) coupled by the parameters $\epsilon_{B,g}^{(01)}$ considerably exceed the corresponding "satellite" harmonics ($E_{m+2,n+5} < E_{m,n}$ and $E_{m-2,n} < E_{m,n+5}$, $E_{m+2,n+5}$ and $E_{m-2,n}$ being coupled with $E_{m,n}$ and $E_{m,n+5}$ due to the presence of the large parameter $\epsilon_g^{(21)}$).

Let us discuss what modes can be expected in W7-AS. Figure 3 presents the Alfvén continuum in the shot #43348, which is calculated with the COBRA code.[2] The dots mark the continuum [they show eigenvalues of Eq. (1) obtained for several chosen values of r/a, where a is the minor radius of the plasma]. The absolute gaps are seen as voids in the

continuum, which are almost horizontal in the plasma core. Such gaps can be considered as envelopes of numerous local gaps arising at avoided crossings of branches $(m,n) = (m_1, n_1)$ and $(m,n) = (m_1 + \mu, n_1 + \nu N)$ for various m_1 and n_1 with the same coupling numbers μ and ν.[2] The upper and lower parts of the continuum are obviously different. The lower part, $\omega \lesssim 200\,\mathrm{kHz}$, resembles the pattern usually observed in tokamaks: Wide bands of the continuum are separated by narrow gaps. In the upper part, $\omega \gtrsim 200\,\mathrm{kHz}$, the situation is just the opposite: The continuum turns into narrow threads squeezed between wide gaps. Each thread consists of numerous continuum branches with $k_\parallel$ of the dominant harmonic varying in the interval $k_\parallel^{(\mu_1\nu_1)} \le k_\parallel \le k_\parallel^{(\mu_2\nu_2)}$, where $k_\parallel^{(\mu\nu)} = |\mu\iota - \nu N|/2$, (μ_1, ν_1) and (μ_2, ν_2) are the coupling numbers of the gaps confining the thread. At the same time, the frequency is almost constant in each thread (at a fixed radius). In each gap, on the contrary, $k_\parallel$ of the dominant harmonics is exactly the same on both "banks" of the gap, $k_\parallel = k_\parallel^{(\mu\nu)}$, where (μ, ν) are the coupling numbers of the gap, whereas the frequency varies considerably.

The shown structure of the continuum can be used to make a conclusion on the existence of GAE modes. In particular, there are reasons to believe that GAEs can hardly appear in the high-frequency part of the spectrum. Indeed, a GAE results from a local extremum of the continuum branch dominated by the harmonic with a certain set of the mode numbers (m,n). If we look at, e.g., the cylindrical continuum branch $(m,n) = (13,3)$ (shown by bold line in Fig. 3), we find that the branch has a minimum at $r/a \approx 0.7$. Thus, we could conclude that a GAE with the frequency about 240 kHz may exist below this minimum. However, the real branch (grey circles in Fig. 3) has nothing to do with the considered cylindrical one. It jumps across the $(2,1)$, $(3,1)$, and $(4,1)$ gaps. As the continuum bands separating these gaps are, actually, lines, the branch follows these lines between the jumps. As a result, it has local extrema only at the radii corresponding to the jumps. Thus, we conclude the GAE modes can hardly exist in the region $\omega \gtrsim 200\,\mathrm{kHz}$. The situation drastically changes in the low-frequency part of the W7-AS spectrum. The continuum bands in this region are relatively wide, and the branches can still have local extrema between the gaps.

The harmonic composition of the waves producing the continuum branches is also qualitatively different in the low-frequency and high-frequency parts of the W7-AS continuum. The harmonic spectrum of several typical branches in different parts of the continuum are presented in Figs. 4 and 5. As was shown in previous publications,[2,16] the solutions of Eq. (1) are invariant of m and n as long as $k_\parallel$ of the wave is fixed. For this reason, the harmonic amplitudes, $|\Psi_{m,n}|$, are shown versus the corresponding longitudinal wave numbers, $k_{m,n}$. For definiteness, we will consider one harmonic of each wave function as "the main harmonic" (in most cases, it will really be the harmonic of the maximum amplitude). Then the harmonic with $k_\parallel = k_{\parallel main} + \mu\iota - \nu N$, where $k_{\parallel main}$ is $k_\parallel$ of the main harmonic, will be referred to as "the (μ, ν) satellite".

Figure 4 shows the wave functions corresponding to frequencies in the interval $0 < \omega \leq 71\,\mathrm{kHz}$ and $k_{\parallel main}$ in the interval $0.01 \leq k_{\parallel main} R_0 \leq 0.38$. One can see that most wave functions are dominated by a single (main) harmonic, the $(-1, 0)$ and $(-2, 0)$ satellites being the most significant. The amplitude of all satellite harmonics is typically several times smaller than that of the main harmonic. The exceptions are some eigenfunctions (for instance, $\omega = 28\,\mathrm{kHz}$ and $\omega = 71\,\mathrm{kHz}$) in which the magnitude of $k_{\parallel main}$ is close to that of the $(-1, 0)$ and $(-2, 0)$ satellites, respectively, and the sign is opposite (which means that the corresponding eigenfrequencies are close to the $(1, 0)$ and $(2, 0)$ continuum gaps, respectively). In these cases, the amplitudes of such two harmonics are close. In general, the wave functions of the continuum branches are, with slight distortions, those of the cylindrical continuum aside from the gaps and solutions of the two-harmonic equation, Eq. (4), near a gap.

The situation is quite different in the upper part of the continuum, see Fig. 5, where some typical continuum wave functions for $215\,\mathrm{kHz} \leq \omega \leq 442\,\mathrm{kHz}$ and $1.725 \leq k_{\parallel main} R_0 \leq 2.075$ [which corresponds to the vicinity of the gaps $(\mu, \nu) = (2, 1)$, $(3, 1)$, and $(4, 1)$], are shown. We observe that the wave functions that have $k_{\parallel main}$ close a gap, i.e., $k_{\parallel main} \approx k_\parallel^{(\mu\nu)}$, look almost symmetric, each having a pair of dominant harmonics of almost equal amplitudes with $k_\parallel = k_{\parallel main}$ and $k_\parallel = k_{\parallel main} - |\mu\iota - \nu N| = -k_{\parallel main}$ and a symmetric set of satellites. In particular, those close to the $(2, 1)$ and $(4, 1)$ gaps ($\omega = 442\,\mathrm{kHz}$ shown

by squares and $\omega = 231\,\mathrm{kHz}$ shown by diamonds, respectively) contain satellites with the amplitude of about 1/3 of the main harmonic pair). The wave functions of two branches located near the $(3,1)$ gap ($\omega = 273\,\mathrm{kHz}$ shown by stars and squares) contain even larger satellites: The $(2,1)$ and $(1,0)$ satellites [the latter are, in fact, the $(-2,1)$ satellites of the $(3,1)$ satellites] are about 80% of the main pair of harmonics. The wave functions with $k_{\|main}$ not corresponding to the boundary of a gap are asymmetric, each having a satellite exceeding 80% and, at least, two satellites exceeding 25% of the main harmonic. (Note that the symmetric and asymmetric wave functions located in the same continuum band have almost the same frequencies because, as mentioned above, continuum branches with different magnitudes of $k_{\|main}$ are squeezed by gaps into thin threads in this part of the spectrum!) In general, the wave functions in this part of the continuum have several (3 or more) considerable Fourier components. One can expect that this property will be inherited by the eigenmodes of the discrete spectrum in this frequency range, which will also be complex compounds of many Fourier harmonics.

Our analysis indicates that the Fourier spectrum of gap modes in stellarators may consist of many considerable harmonics. We will refer to such gap modes as "compound modes". In addition, our analysis shows that there are branches of the continuum with a complicated compound structure, which have asymmetric Fourier spectra but are adjacent to continuum gaps. Therefore, we can suppose that discrete compound modes with asymmetric spectra of $k_{\|}$ can exist in gaps of AC in stellarators. Such compound modes, if they exist, differ from the conventional gap modes, which have symmetric spectra of $k_{\|}$. They perhaps may arise due to the complicated structure of the continuum. Special analysis is required to see whether such unusual modes really exist.

III. RESONANCES BETWEEN THE MODES AND ENERGETIC IONS

The energetic ions drive instabilities of Alfvén eigenmodes through resonance interaction with the modes. The corresponding resonance condition can be written as follows:[3]

$$\omega = (k_{\|} + 2jk_r)v_{\|}, \tag{5}$$

where ω is the mode frequency, $k_r = (\mu_r \iota - \nu_r N)/(2R_0)$; μ_r and ν_r are the "resonance" coupling numbers, i.e., the numbers of the Fourier harmonic of the magnetic field strength that couples the mode with the ions, $j = \pm 1$. The magnitude of ω for a gap mode (we take $\omega > 0$) depends on the location of a corresponding gap in the Alfvén continuum.

Let us consider a mode localized in the vicinity of a certain radius r_* and consisting of only two harmonics with the mode numbers (m, n) and $(m + \mu_0, n + \nu_0 N)$, which are coupled due to the parameters $\epsilon_{B,g}^{(\mu_0 \nu_0)}$. Then we obtain $k_{mn} = k_{mn}(\iota_*) = -k_*$ with $k_* = (\mu_0 \iota_* - \nu_0 N)/(2R_0)$ and $\iota_* = \iota(r_*) = (2n + \nu_0 N)/(2m + \mu_0)$.[1,2] If we approximate the mode frequency as $\omega = |k_{mn}| v_A$, we can find the following resonance velocity for the gap modes:[3]

$$v_\parallel^r = v_{A*} \left(1 + 2j \frac{\mu_r \iota_* - \nu_r N}{\mu_0 \iota_* - \nu_0 N} \right)^{-1} \mathrm{sgn}(k_{mn}). \tag{6}$$

The resonance coupling numbers result from the drift motion of the energetic ions and, thus, are determined by the Fourier harmonics of the magnetic field strength (but they do not depend on the metric tensor).[3] One usually takes $\mu_r = 1$, $\nu_r = 0$, which is justified when the toroidicity ($\epsilon_B^{(10)}$) is the main factor that determines the drift velocity of the energetic ions. However, other factors may be of importance and even dominate in stellarators. In particular, the helical harmonic $\epsilon_B^{(11)}$ well exceeds $\epsilon_B^{(10)}$ in HSR4/18 and HSR5/22. Therefore, the helicity-produced resonance numbers $\mu_r = 1$, $\nu_r = 1$ play an important role in these systems, increasing the growth rate and changing the conditions of instabilities.[3] In general, the "nonaxisymmetric" resonances ($\nu_r \neq 0$) determine the instability growth rate, at least, when $\epsilon_B^{(\mu_r \nu_r \neq 0)} \gg \epsilon_B^{(10)}$, and the absolute values of the resonance velocities for $\mu_r, \nu_r \neq 0$ coincide with the ones for $\mu_r = 1$, $\nu_r = 0$. One can show that the coincidence takes place (to be more specific, $v_\parallel^{r(\mu_r \nu_r)} = -v_\parallel^{r(10)}$) for

$$\mu_0 = \pm(j + \mu_r), \quad \nu_0 = \pm \nu_r. \tag{7}$$

Equation (7) is obtained in assumption that the mode is localized near r_* and consists of only two harmonics with the mode numbers (m, n) and $(m + \mu_0, n + \nu_0 N)$. It follows from Eq. (7) that in a particular case of $\mu_r = 1$ the coupling numbers are $\mu_0 = 0$ and $\mu_0 = 2$ for $\nu_0 = \nu_r$; they are $\mu_0 = 0$ and $\mu_0 = -2$ for $\nu_0 = -\nu_r$.

In general, more than two Fourier harmonics of the perturbation may considerably contribute to gap modes. This implies that there are resonance velocities, which are not described by Eq. (6). In order to find additional resonance velocities, we consider a compound mode with the frequency in the (μ_0, ν_0) gap, which consists of the main couple, $E_{m,n} \Leftrightarrow E_{m+\mu_0,n+\nu_0 N}$ and the satellite couples $E_{m,n} \Leftrightarrow E_{m\pm\mu_s,n\pm\nu_s N}$, $E_{m+\mu_0,n+\nu_0 N} \Leftrightarrow E_{m+\mu_0\pm\mu_s,n+\nu_0 N\pm\nu_s N}$. In this case we can introduce the following characteristic magnitudes of the longitudinal wave number: k_*, $k_{1,2} = [(m \pm \mu_s)\iota_* - (n \pm \nu_s N)]/R_0$, and $k_{3,4} = [(m + \mu_0 \pm \mu_s)\iota_* - (n + \nu_0 N \pm \nu_s N)]/R_0$. Using the equation

$$2m\iota_* = 2n + \nu_0 N - \mu_0 \iota_* \tag{8}$$

we can write $k_{1,2}$ and $k_{3,4}$ as

$$k_{1,2} = -k_* \pm 2k_s, \tag{9}$$

$$k_{3,4} = k_* \pm 2k_s, \tag{10}$$

where $k_s = (\mu_s\iota_* - \nu_s N)/(2R_0)$. It follows from Eqs. (9) and (10) that $k_1 = -k_4$, $k_2 = -k_3$, i.e., there are only two independent longitudinal wave numbers of satellites. We present Eqs. (9) and (10) in the form

$$k_{1,2,3,4} = -j_1 k_* + 2j_2 k_s, \tag{11}$$

where $j_{1,2} = \pm 1$. Then, substituting Eq. (11) into Eq. (5) and writing $\omega = |k_*|v_{A*} + \delta\omega$, where $\delta\omega$ takes into account that the eigenfrequency differs from $\omega_* \equiv |k_*|v_{A*}$, we obtain:

$$v_\parallel^r(\mu_s, \nu_s) = v_{A*}(1 + \delta\omega/\omega_*)\left(-j_1 + 2j\frac{\mu_r\iota - \nu_r N}{\mu_0\iota_* - \nu_0 N} + 2j_2\frac{\mu_s\iota - \nu_s N}{\mu_0\iota_* - \nu_0 N}\right)^{-1}\mathrm{sgn}(k_*). \tag{12}$$

It is convenient to write Eq. (12) as

$$v_\parallel^r(\mu_s, \nu_s) = -v_{A*}(1 + \delta\omega/\omega_*)\left(-j_1 + 2j\frac{k_r}{k_*} + 2j_2\frac{k_s}{k_*}\right)^{-1}\mathrm{sgn}(k_*). \tag{13}$$

Note that when $\mu_s = \nu_s = 0$ and $\delta\omega = 0$, Eq. (13) is reduced to Eq. (6). We will refer to the resonances associated with the satellite coupling numbers (μ_s, ν_s) as "compound resonances" to emphasize that they are relevant to compound modes. These

resonances are especially important in the case when the usual resonance given by Eq. (6) is not efficient. For instance, Eq. (6) gives $|v_\parallel^r| = \infty$ and $|v_\parallel^r| \approx v_A/2$ for the Ellipticity-induced Alfvén Eigenmodes (EAE). On the other hand, the compound resonances caused by toroidicity are $|v_\parallel^r| \approx v_A$, and $|v_\parallel^r| \approx v_A/3$. Because the instability growth rate strongly increases with $v_\parallel^r$, see, e.g., Ref.[3], one can expect that the compound resonance $|v_\parallel^r| \approx v_A$ will mainly contribute to the growth rate when $v_0 > v_A$, where v_0 is the maximum energy of the energetic ions, unless the satellite coupling parameters, $\epsilon_{B,g}^{(\mu_s\nu_s)}$, are very small.

The resonance given by Eq. (5) is responsible not only for the destabilization of gap modes but also for the instabilities of the Energetic Particle Modes (EPM) with the frequencies lying in the Alfvén continuum close to the gaps in the continuum. Using Eqs. (5), (9), and (10), we obtain the frequencies of the EPM modes:

$$\begin{aligned}\omega &= |-j_1 k_* + 2jk_r + 2j_2 k_s| R_0 \iota^{-1} \omega_t \\ &= |-0.5 j_1(\mu_0 \iota_* - \nu_0 N) + j(\mu_r - \nu_r N) + j_2(\mu_s \iota_* - \nu_s N)| \iota^{-1} \omega_t, \end{aligned} \tag{14}$$

where $\omega_t = |v_\parallel| \iota / R_0$ is the transit frequency. For instance, Eq. (14) yields the known result for a toroidicity-induced EPM, $\omega/\omega_t = 0.5$ and $\omega/\omega_t = 1.5$,[22] provided that $\mu_r = 1$, $\nu_r = 0$, $\mu_s = \nu_s = 0$. For the EPM-modes associated with the break of the axial symmetry of the magnetic configuration, Eq. (14) predicts, as expected, the existence of higher frequencies. Taking again $\mu_r = 1$, $\nu_r = 0$, $\mu_s = \nu_s = 0$, we obtain $\omega/\omega_t = 0.5N/\iota$ and $|0.5N/\iota - 2|$ for a helicity-induced EPM with $\mu_0 = 2$, $\nu_0 = 1$ and $\omega/\omega_t = |0.5N/\iota \pm 1|$ for a mirror-induced EPM ($\mu_0 = 0$, $\nu_0 = 1$). The compound resonances with $\mu_s = 1$, $\nu_s = 0$ for an EPM near the EAE gap are $\omega/\omega_t = 1$ and $\omega/\omega_t = 3$, i.e., the frequencies of the ellipticity-induced EPMs exceed those of the toroidicity-induced EPMs by a factor of two.

In order to calculate the instability growth rate with taking into account the compound resonances, one can use the corresponding general expressions obtained in Ref.[2]. Here we restrict ourselves to the case of well-localized modes. Then we can write:

$$\begin{aligned}\gamma_\alpha = &\frac{\pi^2 M_\alpha v_{A*}^2}{8\omega \bar{B}^2 r^2} \sum_{\mu_r,\nu_r,j} \mu_r^2 |\epsilon^{(\mu_r\nu_r)}|^2 \int d^3v \left(|v|^2 + v_\parallel^2\right)^2 \\ &\times \left[|v_\parallel^r| \delta(v_\parallel - v_\parallel^r) + \sum_{s=1,2} \frac{|E_1(k_s)|^2}{|E_1(k_*)|} |v_\parallel^r(\mu_s,\nu_s)| \delta\left(v_\parallel - v_\parallel^r(\mu_s,\nu_s)\right) \right] \hat{\Pi} f_b, \end{aligned} \tag{15}$$

where

$$\hat{\Pi} = M\frac{\partial}{\partial \mathcal{E}} - \frac{M\lambda}{\mathcal{E}}\frac{\partial}{\partial \lambda} + \frac{n}{\omega\omega_B \iota}\frac{1}{r}\frac{\partial}{\partial r}, \tag{16}$$

f_b is the distribution function of the energetic ions, $\mathcal{E}$ is the particle energy, $\lambda = \mu\bar{B}/\mathcal{E}$, $E_1(k_s)$ is a covariant component of the satellite amplitude of the electric field, $j = \pm 1$, $\mu = 1$, $\nu = 0, 1$, and the resonance velocity is given by Eq. (13). Equation (15) generalizes a corresponding equation [Eq. (37)] of the mentioned work by taking into account the harmonic $E(k_s)$.

IV. ESTAFETTE OF RESONANCES DURING NBI EXPERIMENTS ON WENDELSTEIN 7-AS

In NBI experiments on W7-AS the Alfvénic activity was strongly dependent on whether v_b/v_A (v_b is the beam particle velocity, v_A is the Alfvén velocity) is less or more than unity, which was not surprising (and followed from the tokamak theory). But till now it was not clear why in the regime with $v_b > v_A$ a small decrease of the Alfvén velocity strongly changed the character of MHD activity. This was the case in, e.g., the shot #43348, see Fig. 6. In this shot the ratio v_b/v_A varied approximately from 0.5 to 1.8. When v_b/v_A slightly exceeded unity, an Alfvén instability was observed at $\omega \sim 50\,\mathrm{kHz}$. Later, for a larger magnitude of v_b/v_A, the unstable waves were characterized by multiple frequencies in the range of $50 - 250\,\mathrm{kHz}$. After that all the instabilities disappeared, and, finally, when v_b/v_A reached the maximum magnitude (about 1.8), an instability with $\omega \sim 230\,\mathrm{kHz}$ appeared.

We will show that this picture can be understood if we take into account the structure of the Alfvén continuum and that the fast ion drive strongly grows with the particle energy [see Eq. (15)].

The Alfvén continuum calculated with the code COBRA for the W7-AS shot #43348 is shown in Fig. 3. We observe that there are several gaps in Alfvén continuum in the frequency range of $50 - 500\,\mathrm{kHz}$. Discrete eigenmodes which can reside in them or corresponding EPM can be destabilized by injected ions. A necessary condition for the

destabilization is that these ions should satisfy the resonance condition given by Eq. (13). A sufficient condition is that the instability drive should exceed the wave damping. Unfortunately, experimental data provide no information on the radial localization and the mode structure of the instabilities. Therefore, a detailed comparison of the theoretical and experimental results is not possible. On the other hand, due to small magnetic shear and rather flat radial profile of the Alfvén velocity, the dependence of the resonance velocities on the mode localization is rather weak if the mode is localized not very close to the plasma edge, which is, in general, hardly possible (the periphery region is characterized by strong continuum damping). In addition, the concept of the absolute gap[1,2] enables us to make conclusions concerning the possible magnitudes of the destabilized modes without specifying the poloidal and toroidal mode numbers. In order to avoid the specification of the damping mechanisms, we will introduce an adjustable parameter v_{min}, which is the minimum magnitude of the beam velocity required for the fulfillment of the condition $\gamma_\alpha > \gamma_{damp}$. This implies that we assume that the instability is possible only when the resonance velocity lies in the interval

$$v_{min} \leq v_\parallel^r \leq v_0, \tag{17}$$

where v_0 is the maximum velocity of the injected particles.

The obtained picture is shown in Fig. 7. It agrees with the experimentally observed evolution of the MHD activity described above. In the calculations we took $r_*/a = 0.3$ and $v_{min} = 0.9v_0$. The latter assumption seems reasonable because in W7-AS the drive of particles with $v_\parallel = 0.9v_0$ is less than the drive produced by the particles with $v_\parallel = v_0$ by a factor of 2. [This estimate follows from $\gamma_\alpha \propto v_r^7 f_b(v_r)$ and the fact that in W7-AS the dependence f_b on v is rather weak in the range of $26 - 50\,\mathrm{keV}$.] The main resonance velocities were used for all the modes except for the EAE modes, for which the compound resonance with $\mu_s = 1$, $\nu_s = 0$ was used. The resonance numbers $\mu_r = 1$ and $\nu_r = 0$ were chosen because the harmonic $\epsilon_B^{(10)}$ produced by toroidicity is the largest in W7-AS, see Fig. 1 (in contrast to W7-X and the Helias reactors).

We conclude that the experimentally observed temporal evolution of the MHD activity can be explained by an "estafette" of resonances occurring during the variation of the

Alfvén velocity. When $1.05 < v_0/v_A < 1.16$ and $1.587 < v_0/v_A < 1.75$, Eq. (17) is satisfied only for the frequency close to ω_* in the TAE and MAE gaps, respectively. When $1.3 < v_0/v_A < 1.45$, Eq. (17) allows for the multiple frequency activity (EAE, HAE_{21}, etc.). Finally, there are no resonance particles satisfying Eq. (17) for $1.16 < v_0/v_A < 1.25$, which explains the disappearance of the instabilities.

V. ALFVÉN EIGENMODES IN ROTATING PLASMAS

A. Plasma rotation in W7-AS

Experiments with NBI on W7-AS show that the plasma may strongly rotate. The velocity of the toroidal rotation during NBI is maximum near the magnetic axis, where it seems to reach the magnitude about $20\,\mathrm{km\cdot s^{-1}}$.[23] The available information concerning the poloidal rotation is that impurity ions (C^{6+}) rotate with the velocity $v^I_{pol} \sim 10-30\,\mathrm{km\cdot s^{-1}}$ in the region $r = 9 - 15\,\mathrm{cm}$ ($r/a = 0.56 - 0.94$); the velocity is maximum at $r = 15\,\mathrm{cm}$ and very small near the magnetic axis and the plasma edge.[24] If a plasma were rotating poloidally with the same velocity as the impurity ions, the rotation would have a very strong influence on Alfvén eigenmodes. A simple estimate shows that the Doppler frequency shift ($\Delta\omega_{dop} = mv_{pol}/r$) for the mode with $m = 4$ localized around $r = 10\,\mathrm{cm}$ would be more than 64 kHz. But in W7-AS the frequency of TAE modes is about 35 kHz [$\omega_{TAE} \approx v_A\iota_*/(2R_0)$], which is considerably less than 64 kHz! However, one can think that the plasma rotates much slower than the impurities with $Z_I \gg 1$. To see it, we use a simple model consisting of the fluid equations of motion for the bulk plasma ions and the impurities, which yields:

$$u^i_{\perp\vartheta} = u^I_{\perp\vartheta} + u^i_D, \tag{18}$$

where $u^i_D = c(Be_in_i)^{-1}dp_i/dr$ is the ion diamagnetic velocity. All the values in this equation were measured experimentally. However, $u^I_{\perp\vartheta}$ and u^i_D have different signs, and, in addition, their difference is within the experimental error bar, which is rather large. Therefore, we can conclude that $u^i_{\perp\vartheta} \ll u^I_{\perp\vartheta}$, but we cannot evaluate the magnitude of $u^i_{\perp\vartheta}$. The total poloidal velocity is $u_\vartheta = u_{\perp\vartheta} + u_\parallel B_\vartheta/B$. Here the second term is small

because $B_\vartheta/B \ll 1$ unless $u_\parallel$ is very large. Thus, $u^i_\vartheta \approx u^i_{\perp\vartheta} \ll u^I_\vartheta$. But, on the other hand, according to our estimate above, $\Delta\omega_{dop}$ would exceed the frequencies of the eigenmodes in the low-frequency part of the spectrum by a factor of 2 if the plasma rotated with the speed of the impurities.

Therefore, it seems probable that $\Delta\omega_{dop}/\omega_{TAE}$ is less than unity but considerable in the experiments on W7-AS. If so, taking into account the Doppler frequency shift may be of importance for a comparison of experimental observations and theoretical predictions. Note that because of the large aspect ratio of the Wendelstein-line stellarators, the toroidal rotation play a minor role unless $u_\varphi \gg u_\vartheta$.

The estimates above were made in the assumption that $\Delta\omega_{dop}$ is monochromatic. However, any gap mode is characterized by, at least, two pairs of the mode numbers, (m, n) and $(m + \mu_0, n + \nu_0 N)$. Thus, a question arises, what is the Doppler shift for the gap modes? Note that when calculating the Doppler frequency shift in tokamak plasmas, one usually considers only the toroidal rotation. In this case, as all harmonics of a gap mode in an axisymmetric plasma has the same toroidal mode number, $\Delta\omega_{dop}$ is the same as if the mode were monochromatic. It seems that the Doppler shift for the gap modes in either stellarators or tokamaks with poloidally rotating plasmas has not been considered in the literature yet. This will be done in this work on the basis of the equations that will be derived below.

B. Derivation of an equation for Alfvén eigenmodes

At first sight, the simplest way to describe the Alfvén eigenmodes in rotating plasmas is to use the plasma frame, but this is a false impression. First of all, it is not clear what is the plasma frame in the presence of the velocity shear. In addition, even in the case when the velocity shear is absent, the situation is not simple because in the plasma frame the equilibrium magnetic field depends on time. For these reasons, we will use the laboratory frame.

As in Ref.[2], in order to derive an equation for Alfvén eigenmodes, we proceed from the Ampère law

$$\nabla\times\mathbf{B} = \frac{4\pi}{c}\mathbf{j}, \tag{19}$$

from which it follows that

$$\nabla\cdot(j_\parallel\mathbf{b}) + \nabla\cdot\mathbf{j}_\perp = 0 \tag{20}$$

and (see Ref.[2])

$$\frac{4\pi}{c}\widetilde{j}_\parallel = \frac{1}{B_0}\nabla\cdot(B_0\mathcal{K}\widetilde{A} - B_0\nabla_\perp\widetilde{A}), \tag{21}$$

where $\mathbf{b} = \mathbf{B}_0/B_0$, $\widetilde{A}$ is the longitudinal component of the vector potential, $\mathcal{K}$ is the magnetic field line curvature. To obtain Eq. (21), we took $\widetilde{\mathbf{A}}_\perp = 0$ and $\mathbf{B} = \nabla\times(\widetilde{A}\mathbf{b})$ and neglected effects of the plasma pressure. This is justified because the Alfvén waves are characterized by $\widetilde{B}_\parallel \approx 0$.

Using the equations $c\mathbf{E} + \mathbf{u}\times\mathbf{B} = 0$ and $\widetilde{\mathbf{E}} = i\omega\mathbf{b}\widetilde{A}/c - \nabla\widetilde{\Phi}$, we obtain the following equation connecting $\widetilde{A}$ and $\widetilde{\Phi}$:

$$c\nabla_\parallel\widetilde{\Phi} = (i\omega + \mathcal{K}\cdot\mathbf{u_0})\widetilde{A} - (\mathbf{u}_0\cdot\nabla_\perp)\widetilde{A}. \tag{22}$$

Note that because of the plasma rotation the component of $\widetilde{\mathbf{E}}$ along the equilibrium magnetic field is not vanishing:

$$\widetilde{E}_\parallel = -\frac{1}{c}\mathcal{K}\cdot\mathbf{u}_0\widetilde{A} + \frac{1}{c}(\mathbf{u}_0\cdot\nabla_\perp)\widetilde{A}. \tag{23}$$

The perturbed perpendicular current can be found from the equation of the plasma motion, $c\rho d\mathbf{u}/dt = \mathbf{j}\times\mathbf{B}$, as

$$\widetilde{\mathbf{j}}_\perp = \frac{c\rho_0}{B_0}\left\{[\mathbf{b}\times(\tilde{\mathbf{u}}\cdot\nabla)\mathbf{u}_0] - [\mathbf{b}\times(i\omega - \mathbf{u}_0\cdot\nabla)\tilde{\mathbf{u}}] + \frac{\widetilde{\rho}}{\rho_0}[\mathbf{b}\times(\mathbf{u}_0\cdot\nabla)\mathbf{u}_0]\right\} + j_{0\parallel}\frac{\widetilde{\mathbf{B}}}{B_0}. \tag{24}$$

Let us expand each perturbed quantity, $\widetilde{X}$, in a Fourier series as follows:

$$\widetilde{X} = \sum_{m,n}\hat{X}_{mn}, \tag{25}$$

where $\hat{X}_{mn} = X_{mn}\exp(im\vartheta - in\varphi - i\omega t)$. Then

$$\hat{\mathbf{j}}_{\perp mn} = \frac{c\rho_0}{B_0}\left\{-i(\omega - \mathbf{k}\cdot\mathbf{u}_0)[\mathbf{b}\times\hat{\mathbf{u}}_{\mathbf{mn}}] + [\mathbf{b}\times(\hat{\mathbf{u}}_{\mathbf{mn}}\cdot\nabla)\mathbf{u}_0] + e^{im\vartheta - in\varphi}[\mathbf{b}\times(\mathbf{u}_0\cdot\nabla)\mathbf{u}_{mn}]\right.$$
$$\left. + \frac{\hat{\rho}_{mn}}{\rho_0}[\mathbf{b}\times(\mathbf{u}_0\cdot\nabla)\mathbf{u}_0]\right\} + j_{0\parallel}\frac{\hat{\mathbf{B}}_{\mathbf{mn}}}{B_0}, \tag{26}$$

where $\mathbf{k}\cdot\mathbf{u}_0 = mu_0^2 - nu_0^3$. All the terms inside the curly brackets in Eq. (26) are expressed through $\mathbf{u}_{mn}$ except for the last one proportional to $\hat{\rho}_{mn}$. The latter can be expressed through $\mathbf{u}_{mn}$ if we assume that the plasma motion is incompressible, $d\rho/dt = 0$:

$$i(\omega - \mathbf{k}\cdot\mathbf{u})\hat{\rho}_{mn} = (\hat{u}_{mn}\cdot\nabla)\rho_0. \tag{27}$$

In turn, $\hat{\mathbf{u}}_{mn}$ can be presented in terms of the potentials Φ_{mn} and A_{mn} due to the equations

$$\hat{\mathbf{u}}_{mn} = \hat{u}_{\|mn}\mathbf{b} - \frac{c}{B_0}[\nabla\hat{\Phi}_{mn}\times\mathbf{b}] + u_{0\|}\frac{\hat{\mathbf{B}}_{mn}}{B_0}, \tag{28}$$

$$\hat{\mathbf{B}}_{mn} = -\mathbf{b}\times\nabla_\perp\hat{A}_{mn} - \boldsymbol{\mathcal{K}}\times\mathbf{b}\hat{A}_{mn}, \tag{29}$$

and the incompressibility condition,

$$\nabla\cdot(\hat{\mathbf{u}}_{\perp mn} + \hat{u}_{\|mn}\mathbf{b}) = 0. \tag{30}$$

The set of Equations (20), (21), and (26)–(30) describes the Alfvén eigenmodes in rotating plasmas.

For the sake of simplicity, we neglect all the terms associated with the rotation except for a term proportional to $\mathbf{k}\cdot\mathbf{u}$ (which describes the Doppler effect) in Eq. (26). This is justified when

$$\omega \gg \Omega_j, \quad \mathbf{k}\cdot\mathbf{u} \gg \Omega_j, \tag{31}$$

where $j = \vartheta, \varphi$, Ω is the rotation frequency, which implies that the mode numbers are large. For small mode numbers the influence of the plasma rotation on Alfvén eigenmodes is negligible when $\omega \gg \Omega_j$. Due to Eq. (31) we have from Eqs. (22), (28), and (29):

$$[\mathbf{b}\times\hat{\mathbf{u}}_{mn}] = -\nabla_\perp\left(\frac{\omega - \mathbf{k}\cdot\mathbf{u}_0}{k_\|}\right)\hat{A}_{mn}. \tag{32}$$

Substituting Eq. (32) into Eq. (26) and using the latter equation and Eqs. (20) and (21), we obtain the following equation for Alfvén eigenmodes in a rotating plasma:

$$\sum_{mn} i\nabla\cdot\left[\frac{(\omega - \mathbf{k}\cdot\mathbf{u}_0)}{v_A^2}\nabla_\perp\frac{(\omega - \mathbf{k}\cdot\mathbf{u}_0)}{k_\|}\hat{A}_{mn}\right] + B_0\nabla_\|\left[\frac{1}{B_0^2}\nabla\cdot(B_0\boldsymbol{\mathcal{K}}\tilde{A} - B_0\nabla_\perp\tilde{A})\right] + \frac{4\pi}{c}\tilde{\mathbf{B}}\cdot\nabla_\perp\frac{j_{0\|}}{B_0} = 0. \tag{33}$$

C. Effects of rotation: Doppler shift for the gap modes and a rotation-induced gap

If coupling parameters ($\epsilon_{B,g}^{(\mu\nu)}$) were vanishing, Eq. (33) would have a singular point at

$$\omega = \mathbf{k}\cdot\mathbf{u} + jk_{\|}v_A, \tag{34}$$

where $j = \pm 1$, which determines the Alfvén continuum in a plasma cylinder. As we have already mentioned, finite parameters $\epsilon_{B,g}^{(\mu\nu)}$ result in gaps in the Alfvén continuum in the vicinity of the local Alfvén frequency ω_*, at which two cylindrical branches with the mode numbers (m,n) and $(m+\mu, n+\nu N)$ intersect. Writing $\omega_1 = mu^2 - nu^3 + j_1(m\iota - n)v_A/R_0$, $\omega_2 = (m+\mu)u^2 - (n+\nu N)u^3 + j_2[(m+\mu)\iota - (n+\nu N)]v_A/R_0$ and taking $\omega_1 = \omega_2$, we find:

$$\omega_* = mu^2 - nu^3 + \frac{(\mu u_*^2 - \nu N u_*^3) + j_2(\mu\iota_* - \nu N)v_{A*}/R_0}{1 - j_1 j_2}, \tag{35}$$

where the radial coordinate (labeled by "$*$") at which the intersection occurs is determined by

$$\iota_* = \frac{j_1 j_2(n+\nu N) - j_1(\mu u_*^2 - \nu N u_*^3)R/v_{A*} - n}{j_1 j_2(m+\mu) - m}. \tag{36}$$

Note that Eq. (36) does not determine ι_* explicitly because $\mathbf{u}_* = \mathbf{u}(r_*)$. The case of interest is $j_1 j_2 = -1$. Then Eqs. (35) and (36) yield:

$$\omega_* = \frac{|\mu\iota_* - \nu N|}{2}\frac{v_{A*}}{R_0} + \left(m + \frac{\mu}{2}\right)u_*^2 - \left(n + \frac{\nu N}{2}\right)u_*^3, \tag{37}$$

where

$$\iota_* = \frac{2n + \nu N + j_1(\mu u_*^2 - \nu N u_*^3)R_0/v_{A*}}{2m + \mu} \tag{38}$$

with $\mathrm{sgn}(j_1) = \mathrm{sgn}(\nu N - \mu\iota_*)$. When obtaining these equations, we have assumed that $\omega_*(u = 0) > 0$. It follows from Eq. (37) that the Doppler shift for the gap modes is characterized by the mode numbers $m + \mu/2$, $n + \nu/2$, i.e., the difference in the Doppler shift for ω_1 and ω_2 (μu^2, $\nu N u^3$) is "shared" by ω_1 and ω_2. Such sharing is caused by the coupling of the considered cylindrical Alfvén branches. Note that because of the rotation, $k_{mn}(r_*) \neq -k_{m+\mu,n+\nu N}(r_*)$:

$$k_{m,n}|_* = \frac{1}{2R_0}\left[-(\mu\iota_* + \nu N) + j_1(\mu u^2 - \nu N u^3)\frac{R_0}{v_{A*}}\right], \tag{39}$$

$$k_{m+\mu,n+\nu N}|_* = \frac{1}{2R_0}\left[\mu\iota_* + \nu N + j_1(\mu u^2 - \nu N u^3)\frac{R_0}{v_{A*}}\right], \tag{40}$$

The rotation shear affects the radial dependence of the cylindrical Alfvén branches ω_1 and ω_2. It can be especially important for the mode with

$$m = 0.5\mu, \quad n = -0.5\nu N. \tag{41}$$

In this case, $\omega_1 = \omega_2$ for any r in the absence of the plasma rotation [Eq. (38) yields $\iota_* = 0/0$]. The presence of the sheared rotation removes this "degeneracy" and leads to a branch crossing at ι_* determined by the following equation:

$$\mu u_*^2 = \nu N u_*^3, \tag{42}$$

which implies that $\mathbf{k}\cdot\mathbf{u} = 0$ and, thus, $\omega_* = |k^{\mu\nu}(r_*)|v_{A*}$, as in the case of $\mathbf{u} = 0$, but with r_* determined by Eq. (42). Equation (42) is essentially a condition of resonance between the poloidal and toroidal rotations. This becomes clear if we take into account that $u^2 \equiv \Omega_\vartheta$ and $u^3 \equiv \Omega_\varphi$ are the frequencies of the poloidal and toroidal rotation, respectively. In the presence of the corresponding coupling parameters, $\epsilon_{B,g}^{(\mu\nu)}$, a gap caused by the rotation may arise in the Alfvén continuum provided that the magnetic shear is sufficiently small.

VI. EFFECT OF LARGE COUPLING PARAMETERS ON GAP MODES

As we already mentioned, in advanced stellarators strong plasma shaping results in large coupling parameters (for instance, $\epsilon_g^{21} \approx 0.8$ in HSR4/18). On the other hand, the magnetic shear in Wendelstein-line stellarators is low, $\hat{s} \sim 0.1$. In this case one can expect that coupling terms not containing second radial derivatives will be of importance. In fact, an attention to this fact was drawn in Refs.[25,26], where AEs in tokamaks were analyzed. According to Ref.[25], small shear leads to appearance of multiple TAEs. In Ref.[26] it was shown that EAE modes at small shear also become multiple but, in contrast to TAE, exist only in the upper part of the gap. These facts indicate that the equations for AEs in stellarators derived in Ref.[1,2] (where the well-known approach[21] consisting in

taking into account only those coupling terms that contain the second radial derivative of the wave function was used) should be amended. This should be done, at least, for the eigenmodes residing in wide gaps produced by the plasma elongation. Below we will derive and analyze an equation for such AEs.

Different Fourier harmonics in an Alfvén eigenmode are coupled due to the dependence of the magnetic field strength and the metrics on the angular variables, ϑ and φ. The angular variation of B and g^{11} is the most important, accounting for the appearance of the continuum gaps and the properties of the continuum in general. However, the angular dependence of two other components, g^{12} and g^{22}, also contributes to the harmonic coupling (the contribution of the components g^{13}, g^{23}, and g^{33} to the Alfvén wave equation is negligible in large-aspect-ratio devices). Expanding g^{12} and g^{22} in Fourier series,

$$g^{12} = \bar{g}^{12}\frac{1}{2}\sum_{\mu,\nu=-\infty}^{\infty}\epsilon_{12}^{(\mu\nu)}\exp(i\mu\vartheta - i\nu N\varphi), \tag{43}$$

$$g^{22} = \bar{g}^{22}\left[1+\frac{1}{2}\sum_{\mu,\nu=-\infty}^{\infty}\epsilon_{22}^{(\mu\nu)}\exp(i\mu\vartheta - i\nu N\varphi)\right], \tag{44}$$

where $\bar{g}^{22} = \bar{\delta}\bar{B}/(2\psi)$ is the approximate flux-surface average of g^{22}, $\bar{g}^{12} = \bar{\delta}\bar{B}$, we obtain two additional sets of coupling parameters, $\epsilon_{12}^{(\mu\nu)}$ and $\epsilon_{22}^{(\mu\nu)}$, satisfying the relationships $\epsilon_{12}^{(-\mu,-\nu)} = \epsilon_{12}^{(\mu\nu)*}$, $\epsilon_{22}^{(-\mu,-\nu)} = \epsilon_{22}^{(\mu\nu)*}$. In our previous works[1,2] the terms containing $\epsilon_{12}^{(\mu\nu)}$ and $\epsilon_{22}^{(\mu\nu)}$ were disregarded. This approximation is usually satisfactory when the coupling parameters are less than the magnetic shear.

We neglect the plasma pressure and the equilibrium current and take $\mathbf{u}_0 = 0$. Then Eq. (33) can be written as follows:

$$\omega^2\nabla\cdot\left(\frac{1}{v_A^2}\nabla_\perp\Phi\right) + B\nabla_\parallel\left\{\frac{1}{B^2}\nabla\cdot\left[B^2\nabla_\perp\left(\frac{1}{B}\nabla_\parallel\Phi\right)\right]\right\} = 0, \tag{45}$$

which is the same as Eq. (9) of Ref.[2] or Eq. (1) of Ref.[25]. In the flux coordinates (x^1, x^2, x^3) Eq. (45) takes the form

$$\omega^2\nabla_j\left(\frac{\sqrt{g}}{\bar{v}_A^2 h_2}g_\perp^{jk}\nabla_k\Phi\right) + \frac{1}{G}\hat{L}\nabla_j\left[Gg_\perp^{jk}\nabla_k\left(\frac{1}{G}\hat{L}\Phi\right)\right] = 0, \tag{46}$$

where g is the determinant of the metric tensor, $G(r) = \sqrt{g}|B|^2 = B_3 + \iota B_2$ is a weak function of r, $g_\perp^{jk} = g^{jk} - B^jB^k/|B|^2$.

Considering an eigenmode residing in the (μ,ν) gap, we assume that only two Fourier harmonics with the mode numbers $(m,n)=(m_1,n_1)$ and $(m,n)=(m_2,n_2)=(m_1+\mu, n_1+\nu N)$ are significant in the Fourier expansion of Φ:

$$\Phi = \Phi_1 \exp(im_1\vartheta - in_1\varphi) + \Phi_2 \exp(im_2\vartheta - in_2\varphi). \tag{47}$$

Here we restrict ourself to the case of $(\mu,\nu)=(2,0)$, $(2,1)$, ans $(2,2)$. The corresponding harmonics of the magnetic field in advanced stellarators of the Wendelstein-line are negligible, and those of the metric tensor weakly depend on the radius and are well described by the paraxial approximation. Using paraxial expressions for the metric tensor[1,2], we obtain

$$\epsilon^{2\nu}_{(12)} = i\epsilon_g^{(2\nu)}, \quad \epsilon_{22}^{(2\nu)} = -\epsilon_g^{(2\nu)} \tag{48}$$

for $\nu = 0,1,2$. On substituting Eq. (47) to Eq. (46) and using Eq. (48), the (m_1,n_1) and (m_2,n_2) harmonics of the resulting equation yield:

$$\begin{aligned}
&\frac{1}{r}\frac{d}{dr}\left[r\left(\frac{\omega^2}{\bar{v}_A^2}-k_1^2\right)\frac{d\Phi_1}{dr}\right] - \frac{m_1^2}{r^2}\left(\frac{\omega^2}{\bar{v}_A^2}-k_1^2\right)\Phi_1 \\
&+\frac{\epsilon_g^{(2\nu)}}{2r}\frac{d}{dr}\left[r\left(\frac{\omega^2}{\bar{v}_A^2}-k_1k_2\right)\frac{d\Phi_2}{dr}\right] + \frac{m_1m_2}{r^2}\epsilon_g^{(2\nu)}\left(\frac{\omega^2}{\bar{v}_A^2}-k_1k_2\right)\Phi_2 \\
&+\epsilon_g^{(2\nu)}\omega^2\left[\frac{m_1+m_2}{2r\bar{v}_A^2}\frac{d\Phi_2}{dr} + \frac{m_2}{2r}(\bar{v}_A^{-2})'\Phi_2\right] - \epsilon_g^{(2\nu)}\frac{m_1+m_2}{2r}k_1\frac{d}{dr}(k_2\Phi_2) \\
&-\frac{k_1}{r}(rm_1\iota')'\Phi_1 - \epsilon_g^{(2\nu)}\left[\iota'(m_1\nu N - n_1\mu)\frac{d\Phi_2}{dr} + \frac{k_1}{r}(rm_2\iota')'\Phi_2\right] = 0,
\end{aligned} \tag{49}$$

$$\begin{aligned}
&\frac{1}{r}\frac{d}{dr}\left[r\left(\frac{\omega^2}{\bar{v}_A^2}-k_2^2\right)\frac{d\Phi_2}{dr}\right] - \frac{m_2^2}{r^2}\left(\frac{\omega^2}{\bar{v}_A^2}-k_2^2\right)\Phi_2 \\
&+\frac{\epsilon_g^{(2\nu)}}{2r}\frac{d}{dr}\left[r\left(\frac{\omega^2}{\bar{v}_A^2}-k_1k_2\right)\frac{d\Phi_1}{dr}\right] + \frac{m_1m_2}{r^2}\epsilon_g^{(2\nu)}\left(\frac{\omega^2}{\bar{v}_A^2}-k_1k_2\right)\Phi_1 \\
&-\epsilon_g^{(2\nu)}\omega^2\left[\frac{m_1+m_2}{2r\bar{v}_A^2}\frac{d\Phi_1}{dr} + \frac{m_1}{2r}(\bar{v}_A^{-2})'\Phi_1\right] + \epsilon_g^{(2\nu)}\frac{m_1+m_2}{2r}k_2\frac{d}{dr}(k_1\Phi_1) \\
&-\frac{k_2}{r}(rm_2\iota')'\Phi_2 + \epsilon_g^{(2\nu)}\left[\iota'(m_1\nu N - n_1\mu)\frac{d\Phi_1}{dr} - \frac{k_2}{r}(rm_1\iota')'\Phi_1\right] = 0,
\end{aligned} \tag{50}$$

where $k_j = (m_j\iota - n_j)/R_0$, and we have neglected the radial variations of the coupling parameters and the terms $\sim r^2/R_0^2$, as well as the terms involving ϵ_B and $\epsilon^{(00)}$.

Note that the validity of the two-harmonic approximation is, generally speaking, yet to be proven for very large coupling parameters reaching as high magnitudes as 0.8.

In order to solve the derived equations a new code BOA-E (BOA extended) was developed, which extends the code BOA[1,2] applicable to reduced equations of Refs.[1,2].

Results of the calculations with the BOA-E code for the HAE_{21} modes in HSR4/18 are shown in Figs. 8–11. Figure 8 shows two continuum branches for the mode numbers $(m,n) = (9,7)$ and $(11,11)$ confining a $(\mu,\nu = (2,1)$ gap and the Alfvén spectrum in a homogeneous plasma. We observe multiple discrete eigenmodes below the upper continuum curve. This picture considerably differs from the spectrum obtained with the use of truncated equations.[1,2] The main difference is that the eigenfrequencies in the lower half of the gap disappear. Figure 9 shows the structure of several eigenmodes. All the eigemodes are localized around the point $r/a = 0.4$, where the two cylindrical branches of AC intersect (see Fig. 8). An exception is the eigenfunction that corresponds to the lowest eigenfrequency, which is localized in the periphery region. In order to compare the results of ideal MHD with results allowing for non-ideal effects, the spectrum of the considered HAE_{21} modes was calculated in the resistive MHD approximation, see Fig. 10. The resistive MHD equations derived in Ref.[4] were used. One of the discrete modes with the normalized frequency of ± 1.5574 is clearly seen. This eigenfrequency exactly coincides with the lowest eigenfrequency in Fig. 8. The other eigenfrequencies of Fig. 8 are not well resolved in the resistive calculations. Thus, we infer that resistivity does not affect the real part of the frequency and results only in $\mathrm{Im}(\omega) \neq 0$. In addition to calculations of HAEs in a homogeneous plasma, modes in inhomogeneous plasmas of HSR4/18 were investigated. It was found that inhomogeneity may strongly affect HAE_{21} modes, in agreement with results of Refs.[1,2], tending to kill the modes. Nevertheless, we found that there are modes that survive even in realistically inhomogeneous plasmas. An example of such modes is given in Fig. 11.

VII. SUMMARY AND CONCLUSIONS

This work contributes to the theory of Alfvén eigenmodes and of their destabilization by energetic ions in stellarators and, in addition, suggests an interpretation of Alfvénic activity observed in experiments with neutral beam injection on W7-AS. In fact, it extends

a theory developed by the authors (which is published, in particular, in Refs.[1–3]) to include effects of the compound structure of the gap modes and associated changes of the resonance velocities of the energetic ions, peculiarities of the Alfvén continuum in Wendelstein-line stellarators, plasma rotation, and the large magnitude of the coupling parameters associated with strong plasma shaping. A new code, BOA-E (BOA extended) is developed with the aim to calculate the AEs on the basis of the amended equations for AEs given by Eqs. (49) and (50).

The main conclusions drawn from the work are as follows.

It is shown that a gap mode residing in a (μ_0, ν_0) gap and localized at a certain radius can be considered mainly as a pair of Alfvén waves propagating in opposite directions with equal phase velocities even when $\epsilon_{B,g}^{(\mu_0\nu_0)}$ is less than some other coupling parameter, $\epsilon_{B,g}^{(\mu_s\nu_s)}$, which provides the presence of satellite pairs of waves. Nevertheless, the amplitudes of the satellite waves may be not negligible. We refer to such modes as the "compound modes".

The existence of the so-called "compound" resonances, which determine the interaction between energetic ions and compound gap/EPM modes in the case when the usual resonances are not efficient, is predicted.

The role of the "nonaxisymmetric" sideband resonances ($\nu_r \neq 0$)[3] is analyzed. It is found that they dominate the interaction between energetic ions and AEs, at least, when $\epsilon_B^{(\mu_r\nu_r\neq 0)} \gg \epsilon_B^{(10)}$ and $\mu_0 = \pm(j + \mu_r)$ with $j = \pm 1$, $\nu_0 = \pm\nu_r$.

Instabilities of the Energetic Particle Modes (EPM) are discussed. It is shown that the presence of "nonaxisymmetric" resonances and additional gaps in the Alfvén continuum of stellarators result in a variety of new characteristic frequencies of the EPM modes, ω_{EPM} (in contrast to tokamaks, where there exist only $\omega_{EPM} \lesssim \omega_t/2$ and $\omega_{EPM} \lesssim 3\omega_t/2$, where ω_t is the transit time frequency, in the vicinity of TAE gap[22]).

Attention is drawn to the fact that the upper part of Alfvén continuum in W7-AS significantly differs from the lower part. The latter is formed mainly under the influence of toroidicity and elongation and resembles the continuum in tokamaks. In contrast to this, the upper part is strongly affected by nonaxisymmetric components of the magnetic field strength and complicated plasma shaping. As a result, gaps in the Alfvén continuum

occupy the most of space on the plane (r, ω) above 200 kHz. Furthermore, each single continuum branch has no local minima except for the radial points where the branch jumps across a gap due to coupling with another branch. This fact prevents the existence of the GAE modes, which implies that gap modes or EPMs with the frequencies close to the gaps rather than GAEs can be responsible for the high-frequency Alfvénic activity observed in experiments on W7-AS.

An explanation of varying MHD (Alfvénic) activity observed in the Neutral Beam Injection (NBI) experiments on W7-AS[11] is suggested. Namely, the temporal evolution of the Alfvén velocity leads to an "estafette" of resonances: Depending on the Alfvén velocity, various gap modes (TAE, EAE, HAE_{21}, MAE) or EPM with frequencies in the vicinity of these gaps can be destabilized. At certain magnitudes of v_A, no modes can be in resonance with the ions having the energy about the energy of the injected particles (50 keV), in which case the MHD activity disappears.

Equations for the Alfvén eigenmodes in a rotating plasma are derived. In a practically important case when the frequency of the rotation (poloidal or toroidal) is small in comparison with the mode frequency, the effect of the rotation is important for the modes with high mode numbers. This effect then consists in the Doppler frequency shift, which is "shared" between the harmonics that compose the gap mode. It is found that the shear of the rotation may play an important role, producing a new gap in the continuum. This occurs when there is a resonance between the poloidal and toroidal rotations, $\mu\Omega_\vartheta = \nu\Omega_\varphi$, for the modes for which two cylindrical Alfvén branches coincide in the absence of the rotation, $m = 0.5\mu$ and $n = -0.5\nu N$.

It is shown that when coupling parameters are relatively large, keeping all the terms with these parameters in the equation for AEs is of importance. In particular, it significantly affects the HAE_{21} eigenmodes. A general conclusion of Refs.[1,2] that plasma inhomogeneity tends to kill Alfvén eigenmodes with the global structure is confirmed. But, at the same time, the modes that survive in realistically inhomogeneous plasmas are found.

ACKNOWLEDGMENTS

The authors thank Dr. J. Baldzuhn and Dr. H. Ehmler for discussions of experimental data on plasma rotation in W7-AS. One of the authors (Ya.K.) acknowledges the hospitality of the Max-Planck-Institut für Plasmaphysik in Garching.

The work is carried out within the Partner Project Agreement No. P-034b between the Science and Technology Center in Ukraine, the Institute for Nuclear Research of the Ukrainian Academy of Sciences, and Max-Planck-Institut für Plasmaphysik.

REFERENCES

[1] Ya. I. Kolesnichenko, V. V. Lutsenko, H. Wobig, Yu. V. Yakovenko, and O. P. Fesenyuk, *Alfvén Eigenmodes in Helias Configurations (Part I), IPP Report III/261* (Max-Planck-Institut fr Plasmaphysik, Garching bei München, 2000).

[2] Ya. I. Kolesnichenko, V. V. Lutsenko, H. Wobig, Yu. V. Yakovenko, and O. P. Fesenyuk, Phys. Plasmas **8**, 491 (2001).

[3] Ya. I. Kolesnichenko, V. V. Lutsenko, H. Wobig, and Yu.V. Yakovenko, Phys. Plasmas **9**, 517 (2002).

[4] Ya. I. Kolesnichenko, V. V. Lutsenko, H. Wobig, and Yu.V. Yakovenko, "Alfvén Eigenmodes and Their Destabilization by Fast Ions in Optimized Stellarators", in *Proceedings of the 7th International Atomic Energy Agency Technical Committee Meeting on Energetic Particles in Magnetic Confinement Systems, Göteborg, 2001* (International Atomic Energy Agency, Vienna, 2002), Report IT-9; Nucl. Fusion **42** (2002), invited paper, to be published.

[5] C. Nührenberg, Plasma Phys. Control. Fusion **41**, 1055 (1999).

[6] C. Nührenberg, in *ISSP-19 "Piero Caldirola", Theory of Fusion Plasmas*, edited by J. W. Connor, O. Sauter, and E. Sindoni (Editrice Compositori – Società Italiana di Fisica, Bologna, 2000), p. 313.

[7] N. Nakajima, C. Z. Cheng, and M. Okamoto, Phys. Fluids B **4**, 1115 (1992).

[8] F. Wagner, Transactions of Fusion Technology **33**, 67 (1998).

[9] A. Könies, in *Proceedings of the 7th International Atomic Energy Agency Technical Committee Meeting on Energetic Particles in Magnetic Confinement Systems, Göteborg, 2001* (International Atomic Energy Agency, Vienna, 2002), Report OT-20.

[10] D.A. Spong, B.A. Carreras, and C.L. Hedrick, Phys. Fluids B **4**, 3316 (1992).

[11] A. Weller, M. Anton, J. Geiger, M. Hirsch, R. Jaenicke, A. Werner, W7-AS Team, C. Nührenberg, E. Sallander, and D. A. Spong, Phys. Plasmas **8**, 931 (2001).

[12] O. P. Fesenyuk, Ya. I. Kolesnichenko, H. Wobig, and Yu. V. Yakovenko, Scientific Papers of the Institute for Nuclear Research, No. 4(6) (Institute for Nuclear Research, Kyiv, 2001), p. 105.

[13] K. Appert, R. Gruber, F. Troyon, and J. Vaclavik, Plasma Phys. **24**, 1147 (1982).

[14] D. W. Ross, G. L. Chen, and S. M. Mahajan, Phys. Fluids **25**, 652 (1982).

[15] C. Z. Cheng and M. S. Chance, Phys. Fluids **29**, 3695 (1986).

[16] Ya. I. Kolesnichenko, H. Wobig, Yu. V. Yakovenko, and J. Kißlinger, Scientific Papers of the Institute for Nuclear Research, No. 4(6) (Institute for Nuclear Research, Kyiv, 2001), p. 69.

[17] A. H. Boozer, Phys. Fluids **24**, 1999 (1981).

[18] G. Grieger, Nucl. Fusion Suppl. **3**, 525 (1991).

[19] H. Wobig, C. D. Beidler, J. Kißlinger, E. Harmeyer, and F. Herrnegger, in *Fusion Energy 1998, 17th International Atomic Energy Agency Conference Proceedings, Yokohama, 1998*, Vol. 4 (International Atomic Energy Agency, Vienna, 1999), p. 1235.

[20] C. D. Beidler, E. Harmeyer, F. Herrnegger *et al.*, Nucl. Fusion **41**, 1759 (2001).

[21] J. W. Van Dam, G.-Y. Fu, and C. Z. Czeng, Fusion Technol. **18**, 461 (1990).

[22] L. Chen, Phys. Plasmas **1**, 1519 (1994).

[23] J. Baldzuhn, private communication (2002).

[24] H. Ehmler, K. McCormick, A. John, and W7-AS Team, "Status and development of LI-beam diagnostic at W7-AS", Report at the Heisenberg 2002 Workshop (2002).

[25] J. Candy, B. N. Breizman, J. W. Van Dam, and T. Ozeki, Phys. Lett. A **215**, 299 (1996).

[26] S. E. Sharapov and A. B. Mikhailovskii, in *5th International Atomic Energy Agency Technical Committee Meeting on Alpha Particles in Fusion Research, Abingdon, 1997, Contributed Papers* (International Atomic Energy Agency, Vienna, 1997), p. 129.

FIGURES

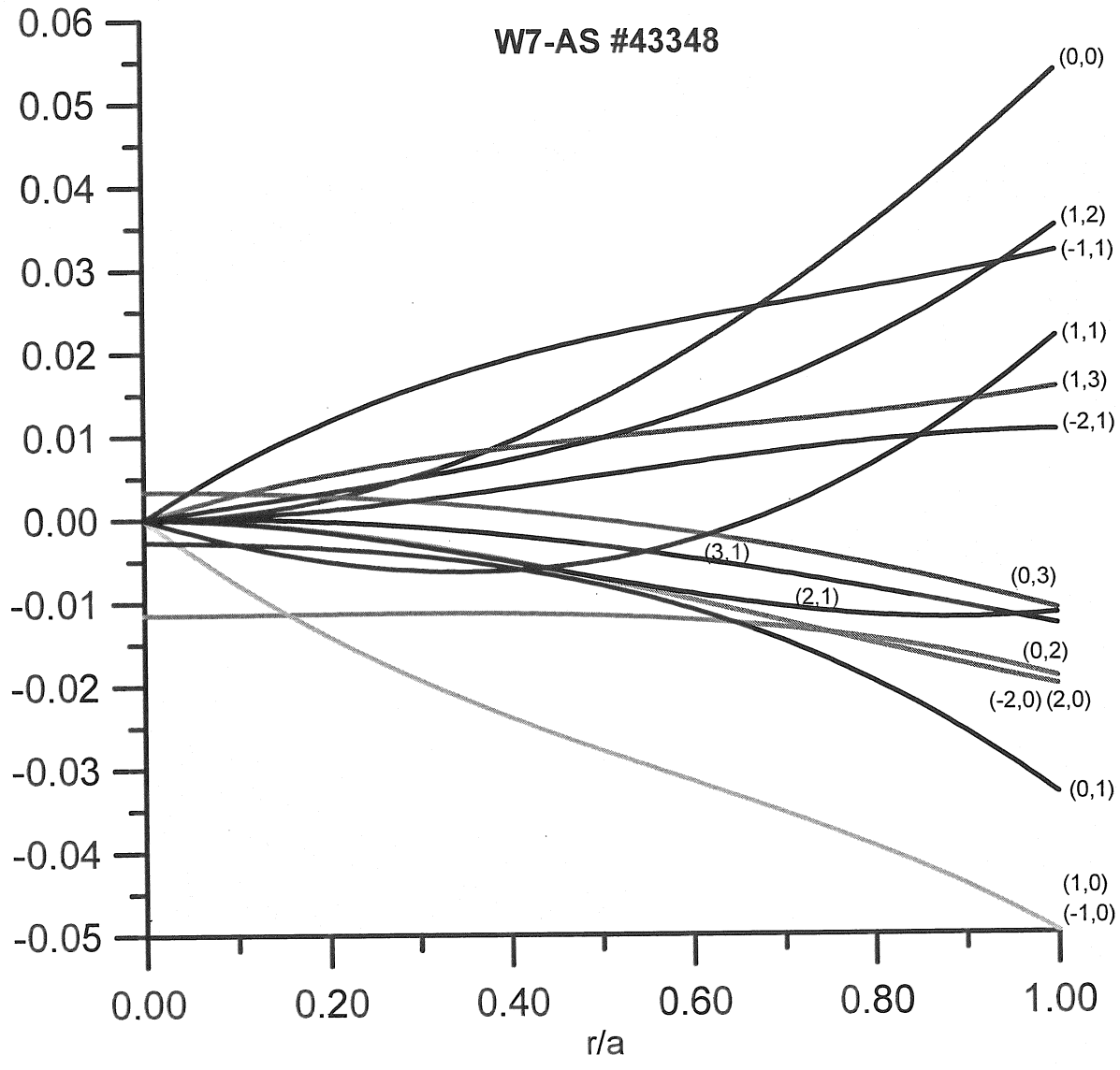

FIG. 1. Main Fourier harmonics, $\epsilon_B^{(\mu\nu)}$, of the magnetic field strength in the shot #43348 of W7-AS. The magnetic field was taken in the form $B = \bar{B}[1 + \frac{1}{2}\sum_{\mu,\nu} \epsilon_B^{(\mu\nu)} \cos(\mu\vartheta - \nu N\varphi)]$ with $\epsilon^{(-\mu,-\nu)} = \epsilon^{(\mu,\nu)}$.

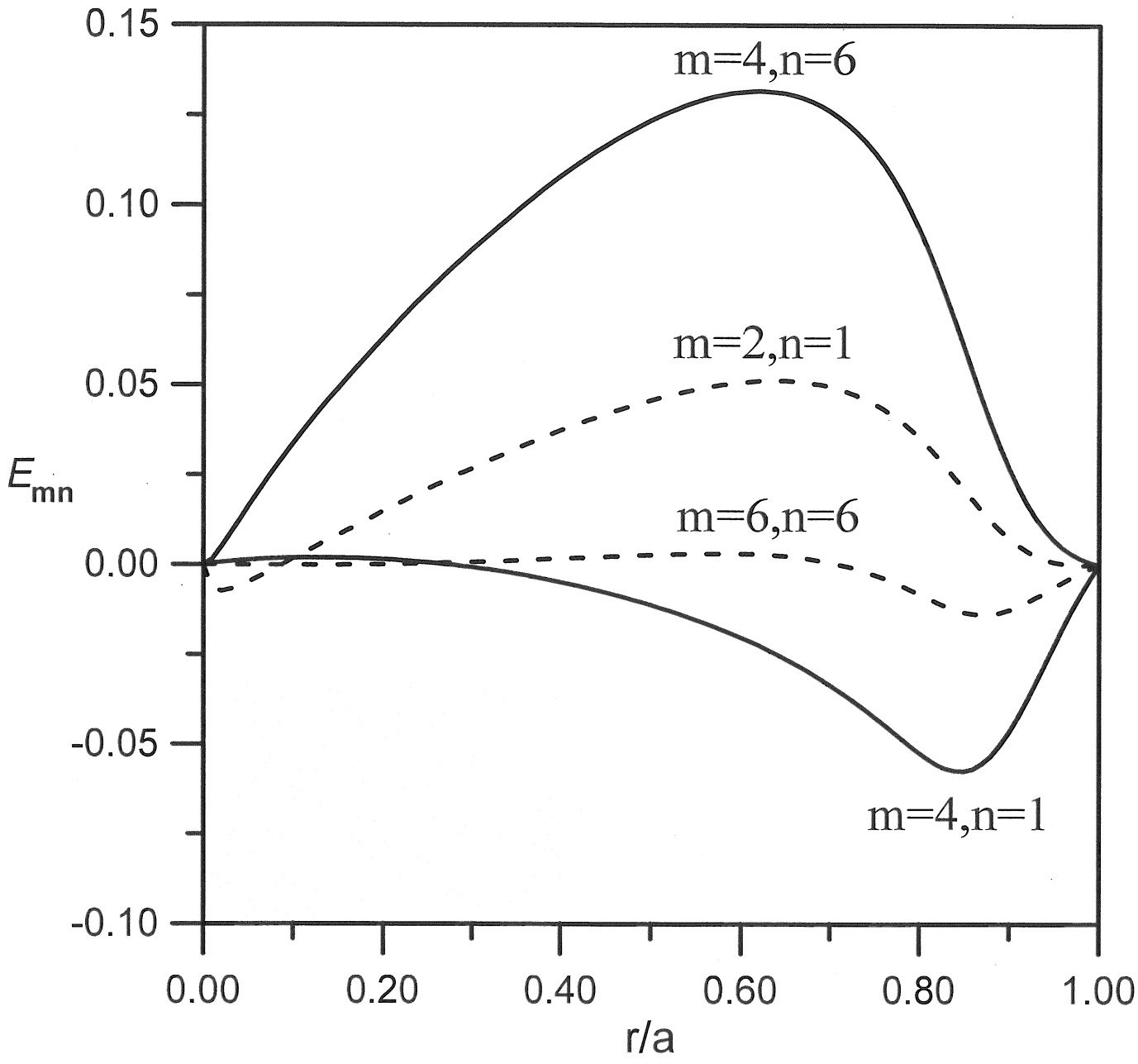

FIG. 2. A compound MAE mode consisting of two main Fourier harmonics (solid lines) and two satellite harmonics (dashed lines) in the Helias reactor HSR5/22. The calculations were carried out with the code BOA.

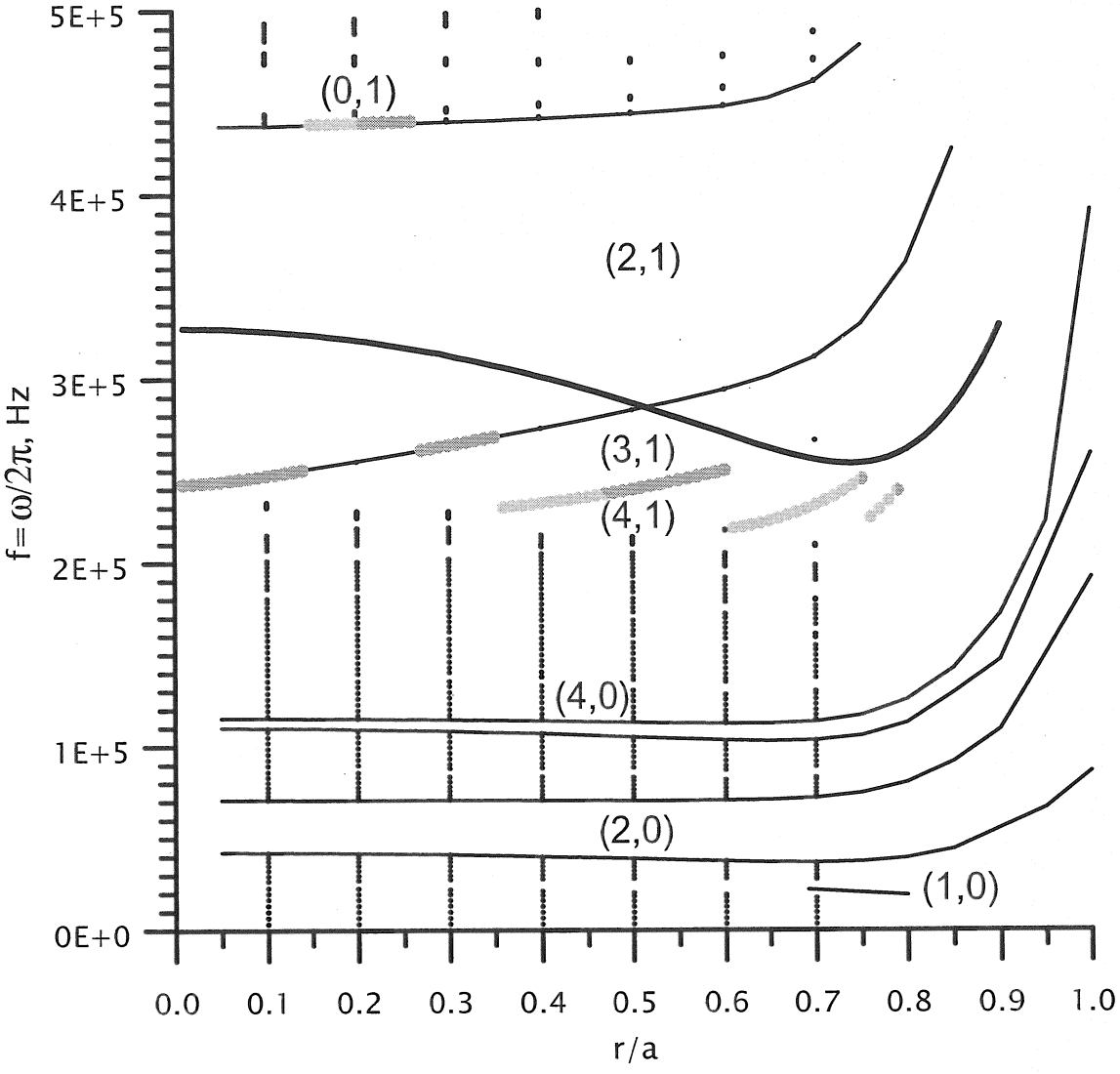

FIG. 3. Calculated Alfvén continuum in the shot #43348 of W7-AS. The gaps are labeled by the coupling numbers (μ, ν) responsible for the formation of each gap. Dots, the calculated frequencies of the continuum spectra for several radii; thin lines, the calculated "banks" of some absolute gaps; grey circles, the continuum branch $(m, n) = (13, 3)$; bold line, the same branch in the cylindrical geometry, i.e., $\omega = (13\iota - 3)\bar{v}_A/R_0$.

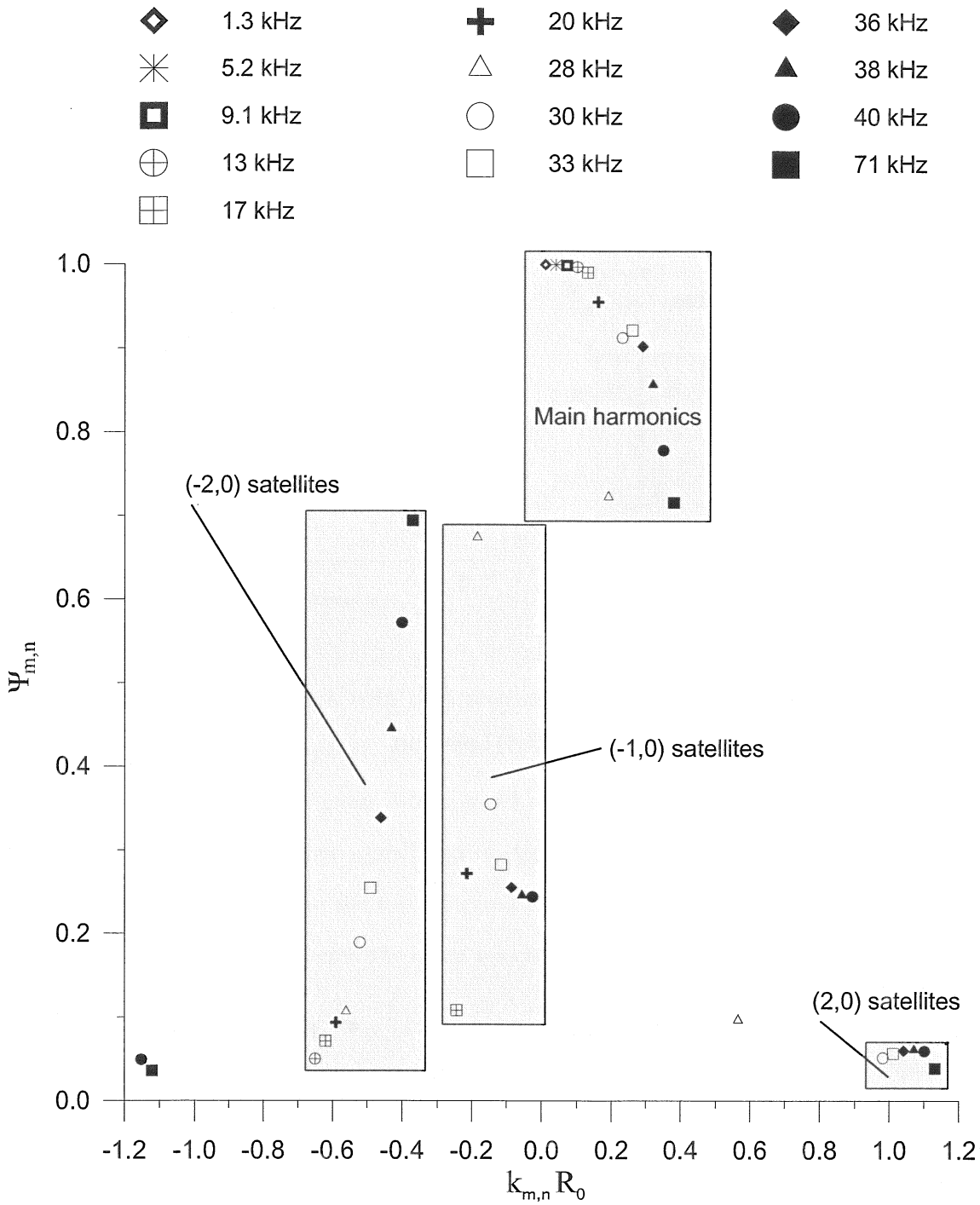

FIG. 4. Fourier spectra of wave functions of the Alfvén continuum in the shot #43348 of W7-AS for $\omega \leq 71\,\mathrm{kHz}$ and $r/a = 0.4$. The harmonics with the amplitude less than 5% of the main one are omitted. The functions are normalized so that the sum of all squared harmonics is unity.

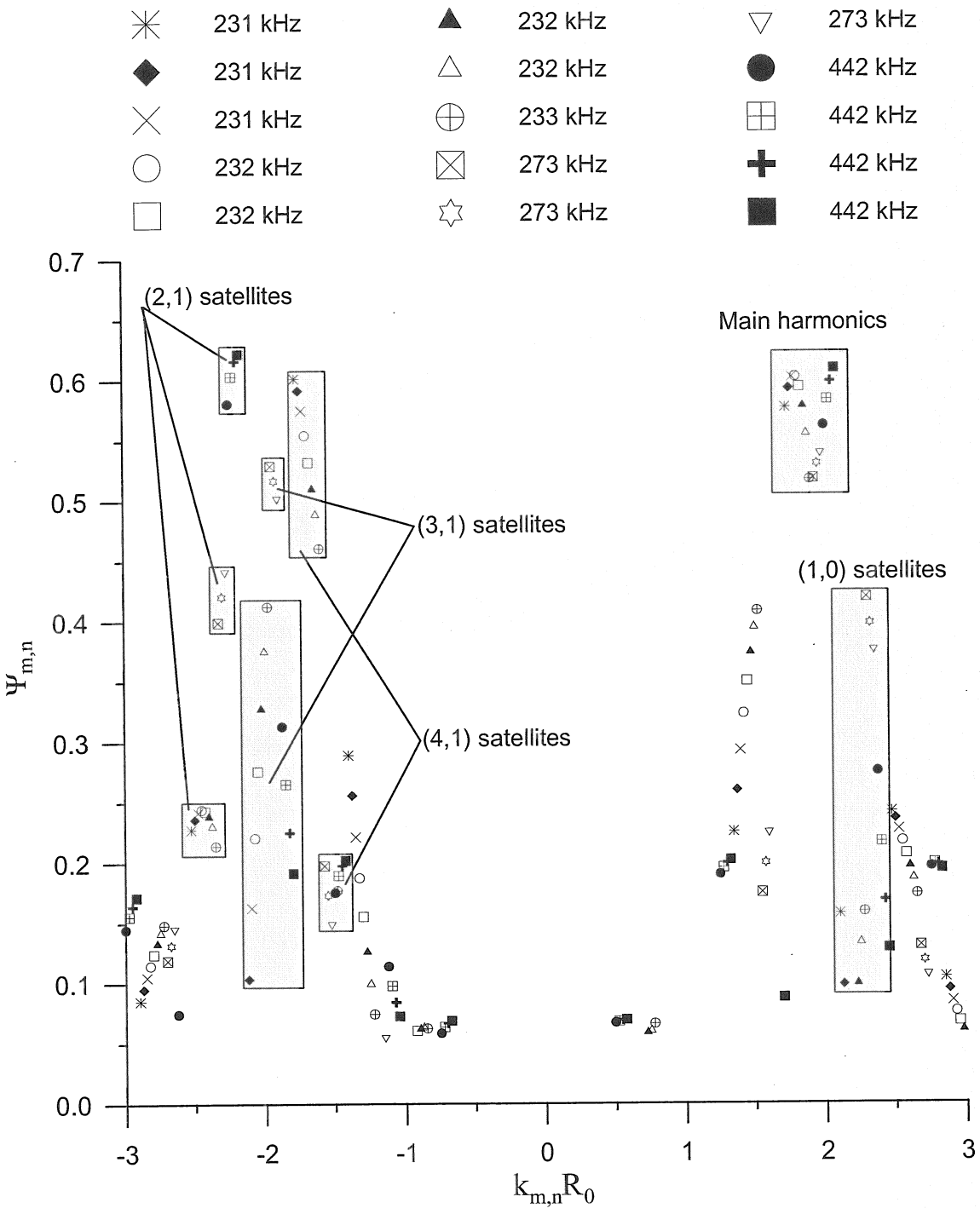

FIG. 5. The same as in Fig. 4 but for $215\,\mathrm{kHz} \leq \omega \leq 442\,\mathrm{kHz}$.

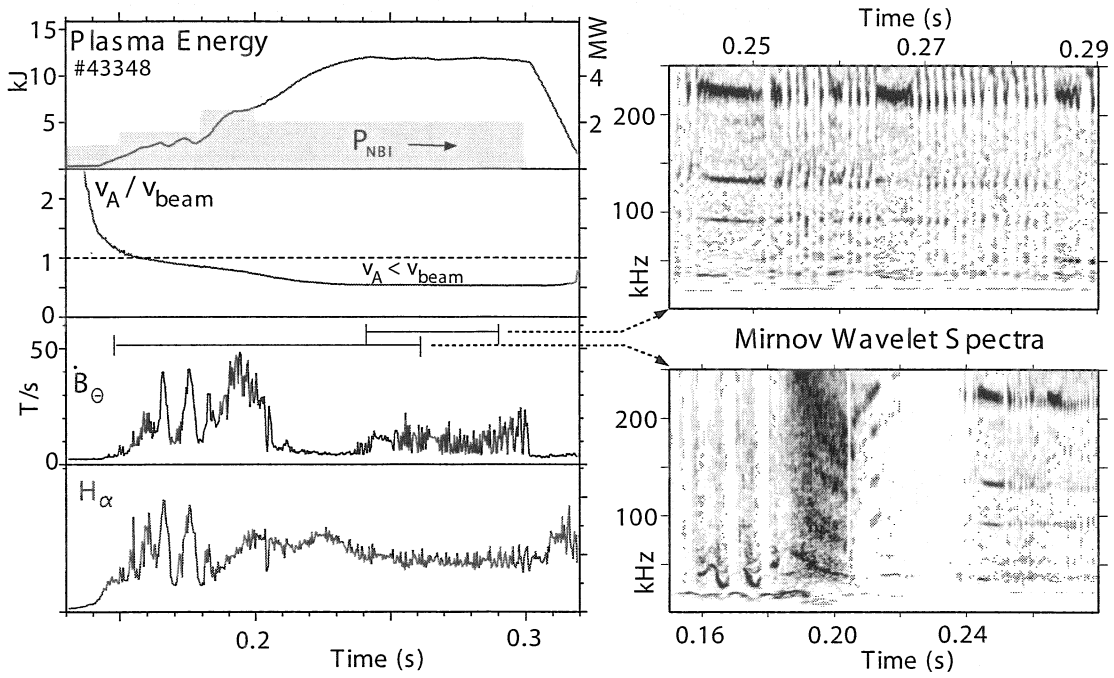

FIG. 6. NBI heated plasma with $\beta(0)$ reaching up to $\approx$ 2.4% (W7-AS shot #43348, $\langle\beta\rangle \leq 1.3\%$) at 1.2 T, $\iota(a) = 0.31$, $n_e \leq 1.1 \times 10^{20}\,\mathrm{m}^{-3}$, Ref.[11]. Left: plasma energy and injected NBI power (shaded), mean Alfvén speed relative to the maximum fast ion velocity, magnetic pickup signal (envelope signal) and H_α signal. Right: wavelet frequency diagram of Mirnov signal corresponding to the two indicated time intervals. The MHD activity appears when the Alfvén speed drops below the beam velocity.

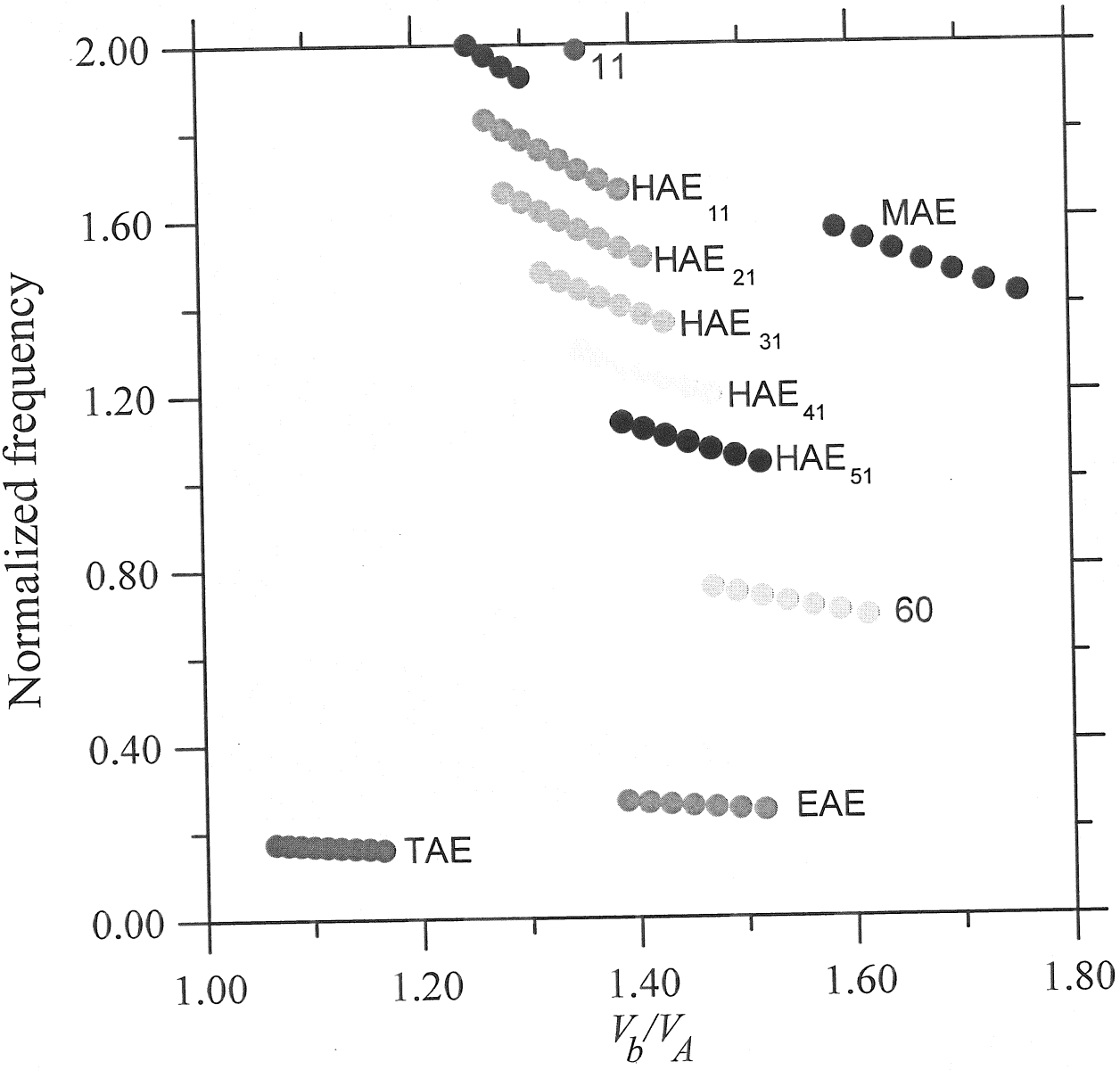

FIG. 7. Theoretically calculated dependence of the destabilized Alfvén spectrum on V_b/V_A in the shot #43348 of W7-AS. This picture agrees with the temporal evolution of Alfvénic activity shown in Fig. 6.

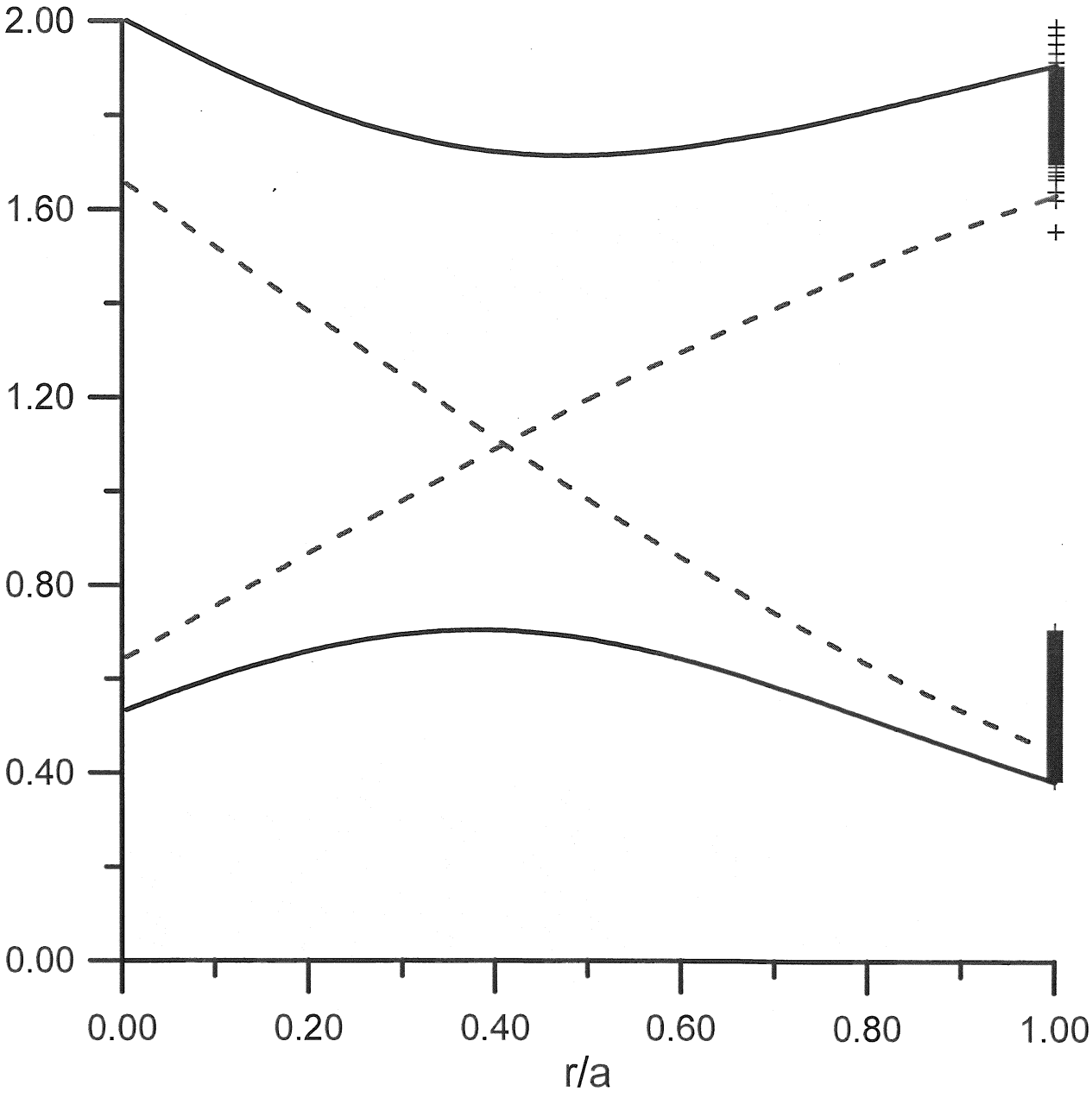

FIG. 8. The HAE_{21} eigenmode spectrum (crosses at $r/a = 1$) and the HAE_{21} gap (solid lines) for the coupled $m = 9$, $n = 7$ and $m = 11$, $n = 11$ harmonics in a homogeneous plasma of the Helias reactor HSR4/18. Dashed lines show the cylindrical continua ($\omega_A = |k_\parallel| V_A$) with the considered mode numbers. There are discrete eigenmodes only in the upper part of the gap; $\lambda_{min} = 1.5574$, $\lambda_{max} = 1.7145$, where $\lambda = \omega R_0 / V_A$ is the normalized eigenfrequency. The calculations were carried out with the code BOA-E.

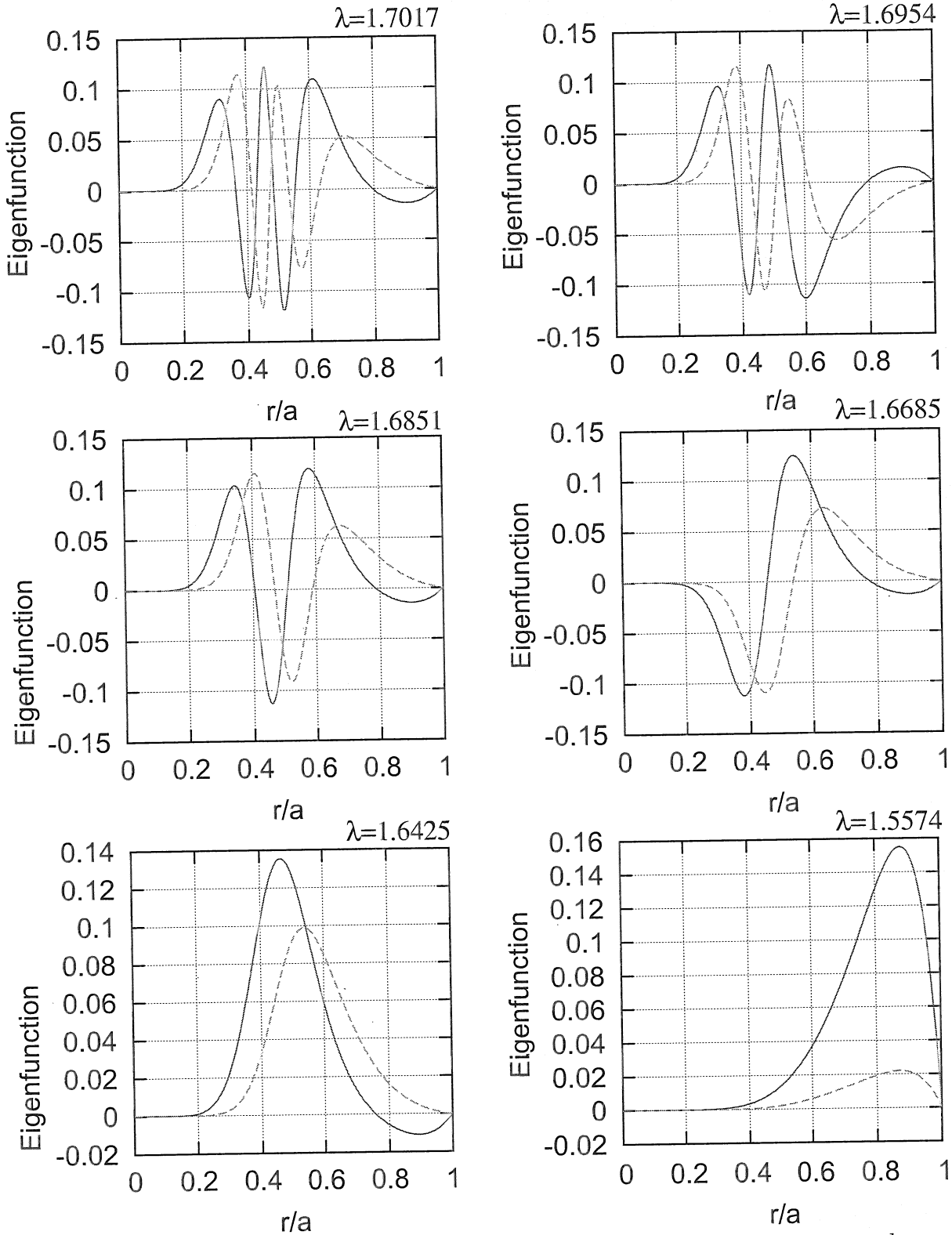

FIG. 9. The radial structure of several HAE_{21} discrete modes. The parameters used are the same as in the Fig. 8. All the modes are localized around $r/a \approx 0.4$, where two cylindrical branches intersect. The exception is the mode with the lowest eigenfrequency ($\lambda = 1.5574$), which is localized at $r/a \approx 0.9$.

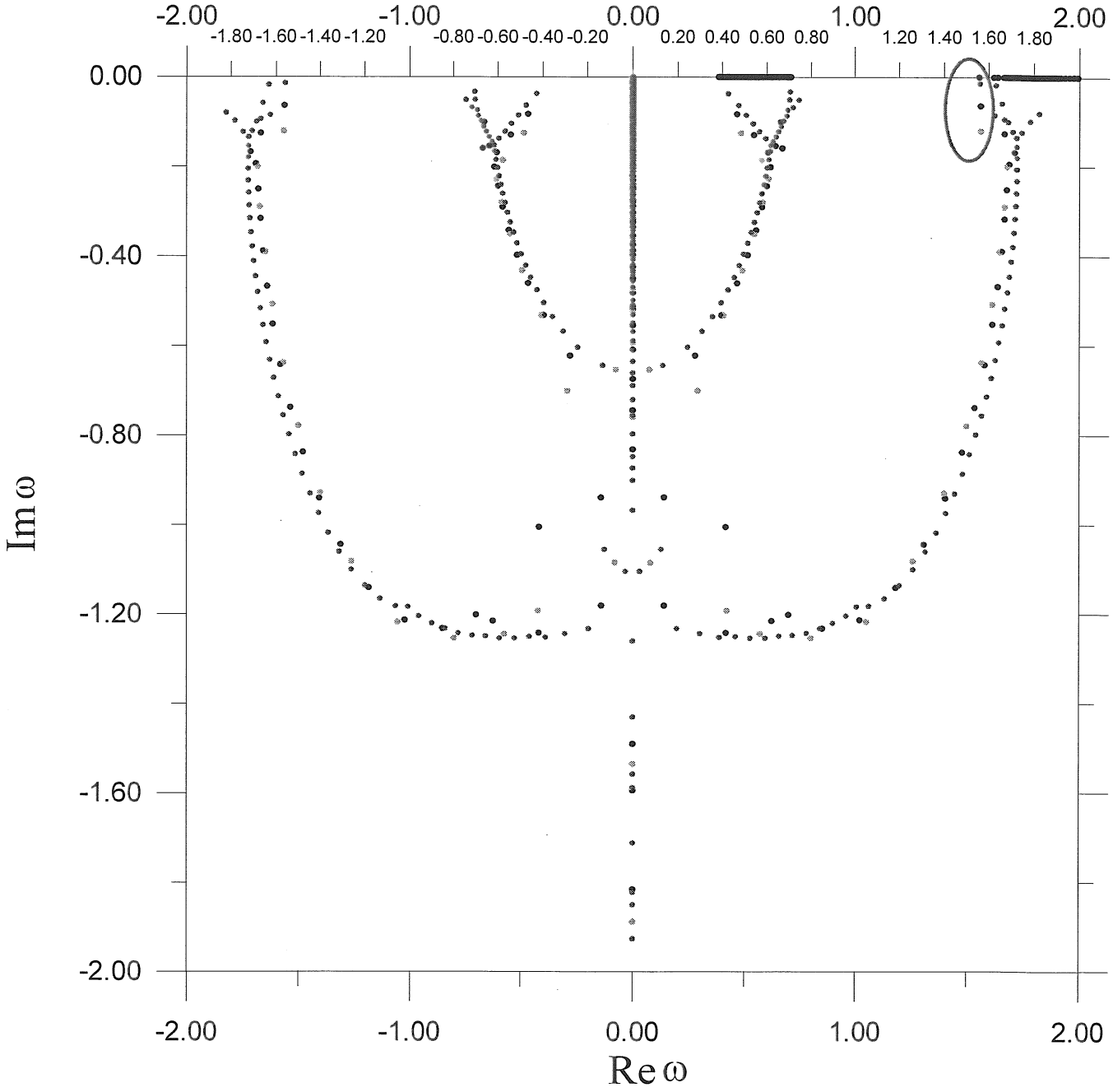

FIG. 10. Resistive MHD spectra (in color) and the ideal MHD spectrum (in black) for HAE_{21} mode with $m = 9, n = 7$ in HSR4/18 with the same parameters as in Figs. 8 and 9. The eigensolution surrounded by the ellipse is a discrete mode with $\mathrm{Re}\,\omega$ coinciding with the lowest eigenfrequency in ideal MHD. The resistive spectra are shown for different values of resistivity η (red colour corresponds to $\eta = 10^{-4}$; blue, $\eta = 5 \cdot 10^{-4}$; green, $\eta = 10^{-3}$).

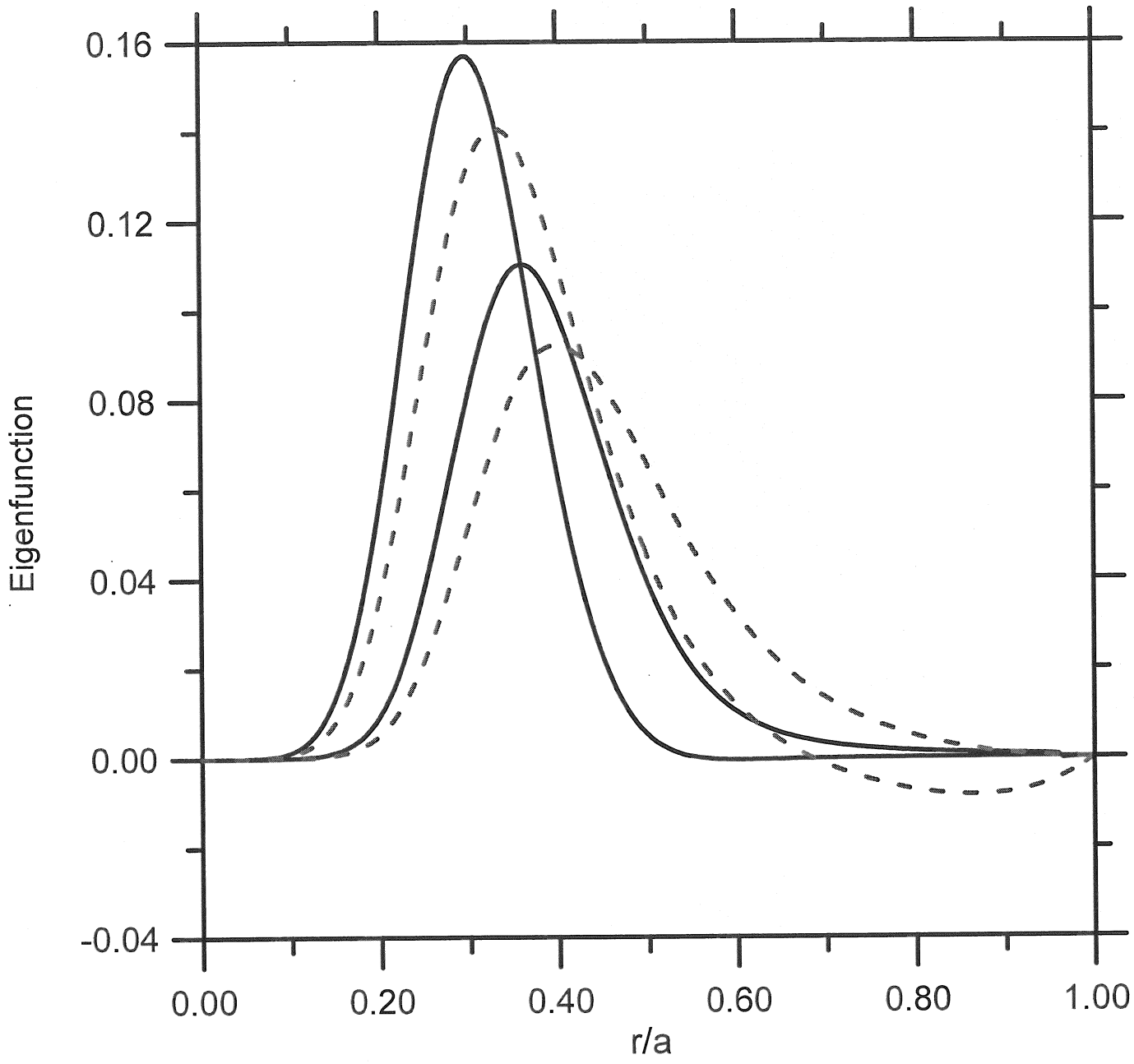

FIG. 11. The radial structure of the HAE_{21} mode with the normalized eigenfrequency $\lambda = 1.6957$ for the coupled $m = 7$, $n = 5$ and $m = 9$, $n = 9$ harmonics in an inhomogeneous plasma (solid lines) and in a homogeneous plasma (dashed lines) of HSR4/18. The radial profile of plasma density was taken in the form $\rho(r) = \rho(0)[1 + r/(x_n a)]^{-1}$ with $x_n = 0.7$. The calculations were carried out with the code BOA-E.